

A Taxonomy of Small Markovian Errors


Robin Blume-Kohout^{1,*}, Marcus P. da Silva,² Erik Nielsen,¹ Timothy Proctor,³ Kenneth Rudinger,¹ Mohan Sarovar,⁴ and Kevin Young³

¹Quantum Performance Laboratory, Sandia National Laboratories, Albuquerque, New Mexico 87185, USA

²Microsoft Quantum, One Microsoft Way, Redmond, Washington 98052, USA

³Quantum Performance Laboratory, Sandia National Laboratories, Livermore, California 94550, USA

⁴Sandia National Laboratories, California, Livermore, California 94550, USA

 (Received 17 March 2021; accepted 29 March 2022; published 13 May 2022)

Errors in quantum logic gates are usually modeled by quantum process matrices (CPTP maps). But process matrices can be opaque and unwieldy. We show how to transform the process matrix of a gate into an error generator that represents the same information more usefully. We construct a basis of simple and physically intuitive elementary error generators, classify them, and show how to represent the error generator of any gate as a mixture of elementary error generators with various rates. Finally, we show how to build a large variety of reduced models for gate errors by combining elementary error generators and/or entire subsectors of generator space. We conclude with a few examples of reduced models, including one with just $9N^2$ parameters that describes almost all commonly predicted errors on an N -qubit processor.

DOI: [10.1103/PRXQuantum.3.020335](https://doi.org/10.1103/PRXQuantum.3.020335)

I. INTRODUCTION

An ideal quantum computation is implemented by a sequence of unitary operations—quantum *logic gates*—applied to a register of qubits. But real quantum processors, in today’s experimental laboratories, are not ideal. Their logic gates are imperfect. Models of these imperfect gates are ubiquitous and essential; they are used to predict the results of running computations [1–5], to measure progress toward specific goals such as fault-tolerant error correction [6–26], and to understand how errors in gates may be reduced [27] or mitigated [28–34]. The standard model of an imperfect quantum logic gate is a *quantum process matrix* specifying a completely positive trace-preserving (CPTP) map [35]. Under certain assumptions (see Sec. III), a process matrix provides a complete description of how the state of the qubits evolves when the gate is applied. But in this role, quantum processes have two critical flaws. They are not easy to interpret, and their complexity grows exponentially with the number of qubits. We present a new representation based on *elementary error generators* that addresses these issues, enabling intuitive and scalable modeling of noisy logic operations.

*rjblume@sandia.gov

Published by the American Physical Society under the terms of the [Creative Commons Attribution 4.0 International](https://creativecommons.org/licenses/by/4.0/) license. Further distribution of this work must maintain attribution to the author(s) and the published article’s title, journal citation, and DOI.

Error generators can model individual one- or two-qubit gates or entire circuit layers that act on a whole quantum processor. Describing noisy gates using error generators makes it transparently easy to partition complex error processes into distinct components with intuitive, physically natural actions. We classify the elementary error generators by their type (see Fig. 1) and then further (Fig. 2) by their weight and support. Partitioning errors in this way enables disaggregating coarse-grained error metrics—e.g., fidelity—to identify exactly how much is contributed by each component (e.g., as in Fig. 3 of Ref. [36]). Error generators also unlock a transformative capability: the design of customized efficient *reduced error models* that capture specific physically motivated subsets of process matrices using exponentially fewer parameters than a full N -qubit process matrix and can be used to model or characterize experimental quantum processors.

II. OUTLINE

Our goal is to analyze and understand small, Markovian gate errors (Sec. III). We begin by representing such errors using *error generators* (Sec. IV). Then, we classify all the error generators that describe small Markovian N -qubit errors (Sec. V). We show that any error generator can be written as a combination of three classes of elementary errors—*Hamiltonian*, *stochastic*, and *active*—that are invariant under unitary changes of basis. We further divide the stochastic error generators into *Pauli-stochastic* and

Sector	Dimension	Action	Example effect (Bloch sphere)	ϵ_L (Error Probability)	θ_L (Error Amplitude)
Hamiltonian \mathbb{H}	$d^2 - 1$	$H_P[\rho] = -i[P, \rho]$		0	1
Stochastic (Pauli) \mathbb{S}	$d^2 - 1$	$S_P[\rho] = P\rho P - \mathbb{1}\rho\mathbb{1}$		1	0
Stochastic (Pauli-correlation) \mathbb{C}	$\begin{matrix} P,Q\rangle=0 \\ P,Q\rangle=1 \end{matrix}$	$C_{P,Q}[\rho] = P\rho Q + Q\rho P - \frac{1}{2}\{P,Q\}\rho$		0	0
	$\begin{matrix} P,Q\rangle=0 \\ P,Q\rangle=1 \end{matrix}$			0	1
Active \mathbb{A}	$\begin{matrix} P,Q\rangle=0 \\ P,Q\rangle=1 \end{matrix}$	$A_{P,Q}[\rho] = i\left(P\rho Q - Q\rho P + \frac{1}{2}\{P,Q\}\rho\right)$		0	1
	$\begin{matrix} P,Q\rangle=0 \\ P,Q\rangle=1 \end{matrix}$			0	0

FIG. 1. We represent an imperfect gate by its *error generator* (Sec. IV) $L = \log(\overline{G}\overline{G}^{-1})$, where G is the process matrix describing the imperfect gate and \overline{G} is the process matrix for the ideal gate. We construct (Sec. V) a useful basis of *elementary error generators* for the vector space \mathbb{L} containing L . This basis defines a taxonomy of small Markovian errors, dividing generators into four sectors (subspaces) shown in this table along with their dimension and their Choi-sum representation. For each sector, we consider the single-qubit case (Sec. VF) and illustrate how the error process generated by a single element from that sector transforms the Bloch sphere. Error metrics that quantify the amount of incoherent and coherent error (see Sec. VII) produced by each elementary generator are tabulated for the generators in each sector and (for $C_{P,Q}$ and $A_{P,Q}$ generators) for the subcases where P and Q anticommute or commute.

Pauli-correlation sectors, which are invariant under Clifford (but not arbitrary) unitaries. We construct a complete basis of elementary error generators for each sector, using one- and two-qubit constructions as constructive examples. We explain the physical origin and impact of each kind of error (Sec. VH) and discuss the relationship between our error generators and the generators of Lindblad master equations (Sec. VI).

After introducing simple metrics of coherent and incoherent error and tabulating them for each elementary error generator (Sec. VII), we show how to further partition those four main sectors into subsectors of fixed *weight* and *support* (Sec. VIII). This fine-grained partition of error generators into physically and logically meaningful classes is the taxonomy promised in the title. We conclude with what we see as the most exciting application of this framework: the construction of customizable, efficient reduced models of errors in N -qubit logic operations that can describe and model specific errors or classes of errors in a quantum processor while minimizing the amount of resources wasted on unlikely or physically implausible errors.

III. SMALL MARKOVIAN ERRORS

We are interested in errors that are (1) small and (2) Markovian. We begin by stating exactly what we mean by these terms. Both represent idealized assumptions that

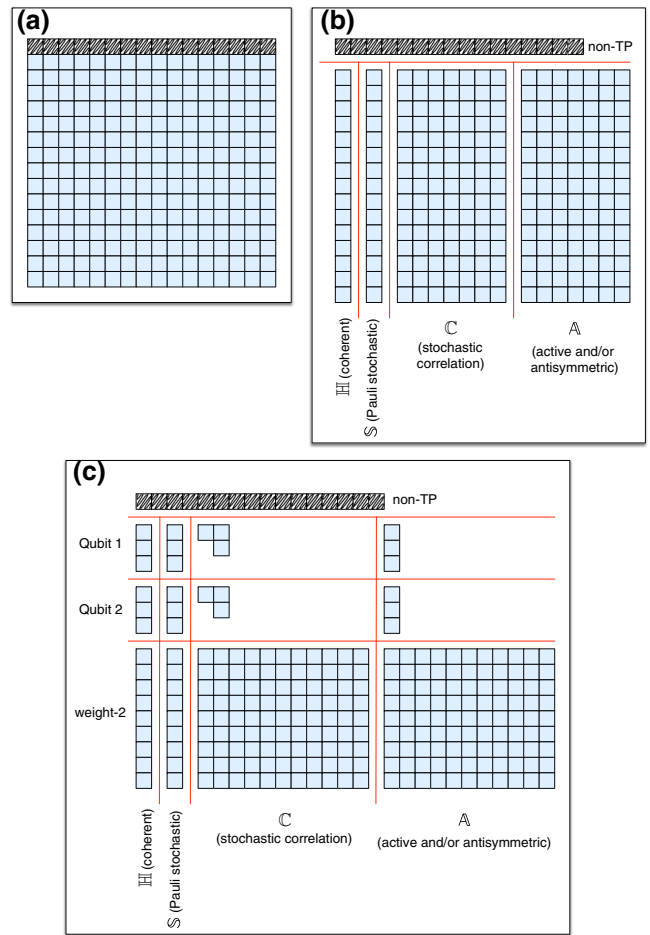


FIG. 2. A two-qubit CPTP map (a) has 240 free parameters (16×16 minus 16 for the top row, which is constrained by trace preservation). It can be reparametrized by its error generator (b), which can be split up into its projections onto \mathbb{H} , \mathbb{S} , \mathbb{C} , and \mathbb{A} sectors. Each of these sectors can be further partitioned (c), following Sec. VIII, into generators with a fixed *weight* (number of qubits on which it acts) and *support* (subset of qubits on which it acts).

never hold exactly in experiments but can be tested experimentally and are often approximately true. Theorems and representations derived in the limit of small Markovian errors can provide accurate approximate results in real-world situations.

A. Definitions

We call a process that changes a system’s state $\rho \rightarrow \rho'$ *Markovian* if, given the nature of the process, ρ' is completely determined by ρ . So if the error associated with a particular gate g is Markovian, then it is described by some map $G_g : \rho \rightarrow \rho'$ that does not depend on the time of day, other gates performed previously, or any other “context” variable. It then follows from the rules of quantum theory that G_g must be linear, completely positive, and

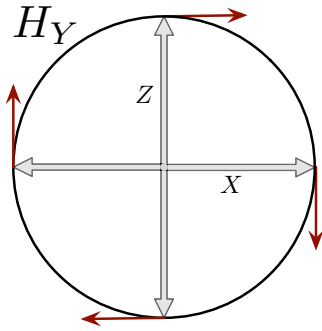


FIG. 3. The action of a representative Hamiltonian error generator. This is how the one-qubit H_Y generator acts on the X - Z plane of the Bloch sphere. It generates rotations, sending $Z \rightarrow X$ and $X \rightarrow -Z$.

trace-preserving—and thus that G_g can be represented by a process matrix. Other definitions of “Markovian” appear in the extensive literature on Markovian and non-Markovian quantum dynamics (see, e.g., Ref. [37] and references therein) but the definition used here is common and we state it explicitly to avoid confusion.

We say that the error in an implemented gate g is *small* if the process matrix G_g that describes its action is close to the “target” process matrix \overline{G}_g that describes an ideal implementation of g . More precisely, we want $G_g - \overline{G}_g$ to be small, so that expressions that are $O([G_g - \overline{G}_g]^2)$ can be neglected. The necessary and sufficient condition is that $\|G_g - \overline{G}_g\|_\diamond \ll 1$. A detailed discussion of the diamond norm can be found in Ref. [38] but the feature most relevant for this purpose is that the diamond norm is the *maximum* of the induced trace distance $\|G_g[\rho] - \overline{G}_g[\rho]\|_1$ over all states ρ on which g could act. If this diamond norm is small, then the action of $(G_g - \overline{G}_g)$ on *all* states is small, which justifies ignoring the action of $(G_g - \overline{G}_g)^2$ on any state. Conversely, if the diamond norm is not small, then there exists some state on which the action of $(G_g - \overline{G}_g)$ is not small and $(G_g - \overline{G}_g)^2$ cannot be ignored.

There is no exact threshold for where $\epsilon_\diamond \equiv \|G - \overline{G}\|_\diamond$ becomes “small.” However, in extensive use we find the following rules of thumb to hold well:

- (a) When $\epsilon_\diamond \leq 0.01$, the techniques and results in this paper work almost flawlessly.
- (b) When $0.01 \leq \epsilon_\diamond \leq 0.1$, we find these techniques (and intuitions based on them) to work reliably if some caution and common sense is applied. For example, if $\epsilon \approx 0.1$, then each second-order $O(\epsilon^2)$ term in $(G_g - \overline{G}_g)^2$ may have magnitude 0.01, and the *combined* impact of several such terms can compete with the first-order term.
- (c) When $\epsilon_\diamond \geq 0.1$, we do not trust error generator analysis except as a qualitative tool, yielding results that

should be confirmed using other methods of analysis that are more appropriate to “large” gate errors.

It follows that this “small Markovian errors” framework *is* appropriate for qubits and quantum processors that approach or exceed theoretical thresholds for fault tolerance (roughly 1% error per gate) but may *not* be useful and reliable for early-stage qubits with gate fidelities much less than 99%.

An additional (and very general) rule of thumb is that any particular error rate of order $O(\epsilon_\diamond^2)$ should not be taken seriously. For example, if the errors in a two-qubit gate are dominated by single-qubit errors of size $\epsilon_\diamond = 0.01$ but error generator analysis suggests the presence of two-qubit correlated errors at rate 10^{-4} , this finding should be taken with a very large grain of salt, because it could (or might not) stem entirely from second-order effects of the single-qubit errors.

B. Superoperators

Consider a logic gate on an N -qubit register. The Hilbert space \mathcal{H} of the N qubits has $d = 2^N$ dimensions and is isomorphic to \mathbb{C}^d . The ideal unitary target gate can be described and represented by a $d \times d$ unitary matrix U that acts on states $|\psi\rangle \in \mathcal{H}$. But noisy evolutions require the richer state space of $d \times d$ density matrices ρ , in which pure states ($\rho = |\psi\rangle\langle\psi|$) and unitary evolution ($\rho \rightarrow U\rho U^\dagger$) are special cases. More generally, $\rho \rightarrow G[\rho]$, where G is a *completely positive trace-preserving linear map* on operators (or “CPTP map” for short). To represent and analyze this action, we can represent ρ by a column vector $|\rho\rangle\rangle$ in the d^2 -dimensional space $\mathcal{L}(\mathcal{H})$ of $d \times d$ matrices. Equipped with the inner product

$$\langle\langle A|B\rangle\rangle \equiv \text{Tr}(A^\dagger B), \tag{1}$$

this is called *Hilbert-Schmidt space*. Now, the gate can be represented by a $d^2 \times d^2$ matrix that acts by matrix multiplication on $|\rho\rangle\rangle$:

$$|\rho\rangle\rangle \rightarrow G|\rho\rangle\rangle. \tag{2}$$

This representation of G is associative—the consecutive application of G and then H is described by HG —and has been called the *superoperator*, *transfer matrix*, or *Liouville representation*.

G can be represented in any orthonormal basis of matrices. We use the N -qubit Pauli basis [39] $\mathcal{P} = \{P_1 \dots P_d\}$. It comprises all N -fold tensor products of the single-qubit Pauli group $\{\mathbb{1}, X, Y, Z\}$. They are all Hermitian. For every N , $P_1 = \mathbb{1}$ and all the rest are traceless. The orthonormality relation is $\text{Tr}(PQ) = d\delta_{P,Q}$ for all $P, Q \in \mathcal{P}$. Every pair of N -qubit Paulis either commutes ($\{P, Q\} = 0$) or anti-commutes ($\{P, Q\} = 0$) and each Pauli except $\mathbb{1}$ commutes

with exactly half the other Paulis and anticommutes with the rest.

An N -qubit superoperator G written in this basis is a $4^N \times 4^N$ matrix [40] with elements

$$G_{P,Q} = \langle\langle P|G|Q \rangle\rangle = \text{Tr}(PG[Q]). \quad (3)$$

A CPTP superoperator must preserve Hermiticity. Since Paulis are Hermitian, G is a real matrix with 16^N free parameters. The constraint of complete positivity (CP) defines a cone [41] but does not reduce the dimension, so a CP map still has 16^N mostly free parameters. A trace-preserving (TP) map satisfies $G^T[\mathbb{1}] = \mathbb{1}$, so its top row must be $[1, 0, \dots, 0]$ and CPTP maps have $4^N(4^N - 1)$ free parameters. A map G is called *unital* if $G[\mathbb{1}] = \mathbb{1}$, and G is unital if and only if its leftmost column is $[1, 0, \dots, 0]^T$.

IV. ERROR GENERATORS

When G describes an imperfect gate, we are less interested in G itself than in how it differs from its unitary target \bar{G} . So we focus on the set of possible small deviations from \bar{G} . This set is different for each \bar{G} , but we can remove the variation by modeling an imperfect gate as its ideal unitary followed by a *post-gate error process*,

$$G = \mathcal{E}\bar{G}. \quad (4)$$

Now, $\mathcal{E} \equiv G\bar{G}^{-1}$ faithfully represents the error in G , and it is always close to the identity process $\mathbb{1}$ when G is close to \bar{G} . This transformation has been suggested and explored by Korotkov in Ref. [42] and deployed experimentally by Rodionov *et al.* in Ref. [43]. The framework we construct here takes advantage of some ideas that first appeared in those papers.

If $\mathcal{E} = \mathbb{1}$, then the gate is perfect. Small errors correspond to small deviations from $\mathbb{1}$. To isolate that deviation, we can compute $\mathcal{E} - \mathbb{1}$ or $\log \mathcal{E}$. These expressions become identical in the limit $\mathcal{E} \rightarrow \mathbb{1}$, since

$$\log X = (X - \mathbb{1}) + O[(X - \mathbb{1})^2], \quad (5)$$

but there are subtle and interesting differences, which we revisit in Sec. VI. For now, we choose the logarithm. \mathcal{E} is a real matrix and, for small errors, it is close to $\mathbb{1}$. Therefore, it has a real logarithm [44]. We define the *post-gate error generator* for G as

$$L = \log(\mathcal{E}) \Leftrightarrow G = e^L \bar{G}. \quad (6)$$

L is a faithful representation of the error in G . But unlike G itself, its magnitude and nature directly represent the magnitude and kind of errors in G . It generates errors after \bar{G} in the same sense that a Hamiltonian H generates a unitary $U = e^{iH}$ [45].

It would be equally valid (and completely equivalent) to write $G = \bar{G}\mathcal{E}'$, and use pre-gate error processes and error generators $L' = \log(\mathcal{E}')$. (A representation using *both* pre- and post-gate error processes has been proposed by Wallman [46].) We use post-gate error generators because it is slightly more intuitive to imagine the error process occurring after the gate, rather than before it.

But this highlights another possible choice: we could compute a *during-gate error generator* L'' by writing $G = \exp(\log \bar{G} + L'')$. This representation works equally well for some errors and it is physically well motivated if G is implemented by a simple pulse. But unlike the pre- and post-gate generators, it is not always a faithful representation of arbitrary errors. Some noisy processes $G \approx \bar{G}$ have no during-gate error generator. For an example, let $\bar{G}[\rho] = Z\rho Z$ perform a single-qubit Z_π rotation and let $G = \mathcal{E}_{pX}\bar{G}$, where $\mathcal{E}_{pX}[\rho] = (1-p)\rho + pX\rho X$ causes a stochastic X error with probability $p > 0$. Now, \bar{G} has two -1 eigenvalues (corresponding to the Pauli X and Y matrices) that form a Jordan block of size 2, so it has a real logarithm. But the stochastic X error process breaks this symmetry in G , which has two *distinct* negative real eigenvalues and therefore has no real logarithm at all [47].

The post-gate error generator avoids this problem. It is the logarithm of a real matrix close to $\mathbb{1}$, so it has no negative eigenvalues and a real L always exists. We emphasize, however, that the post-gate error generator is not intended to model the exact mechanism that generates errors in G . In many systems, gates are implemented by complex pulses with strongly time-varying characteristics and complicated error mechanisms. The error generators we consider here are a mathematical representation of their *effects*, not necessarily of their cause.

We work with generators instead of processes because switching representations changes the meaning of linear combination in a subtle and useful way. Linear combination is natural for both processes and generators but linear combinations of processes are *convex* combinations, aka mixtures. $(\mathcal{E}_1 + \mathcal{E}_2)/2$ means “Flip a coin and perform \mathcal{E}_1 or \mathcal{E}_2 .” In contrast, linear combinations of generators indicate *composition*. If H_1 and H_2 are Hamiltonians, then $H_1 + H_2$ means “Apply H_1 and H_2 ” and it generates a unitary operation, not a mixture of unitaries. Although composition and mixture converge in the small-error regime, generator space admits a clean partition into subspaces representing distinct (and potentially concurrent) error mechanisms, in a way that the convex set of processes does not.

V. A TAXONOMY OF ERROR GENERATORS

L presents the same information as G , but it is more amenable to analysis. Error generators can be dissected into a list of easily interpretable terms. Whereas quantum processes such as G form a *semigroup* [45], generators

such as L form a Lie *semialgebra* [48] that is the solid tangent cone [49] to the set of CPTP maps at $\mathbb{1}$. Its linear closure is a $d^2(d^2 - 1)$ -dimensional vector space that we call *generator space* (\mathbb{L}).

We can construct a basis for \mathbb{L} in which each element has a simple interpretation and produces a recognized quantum logical error. We call these *elementary generators*. They fall into four classes that define subspaces of \mathbb{L} . We denote these subspaces by \mathbb{H} , \mathbb{S} , \mathbb{C} , and \mathbb{A} [see Figs. 2(a) and 2(b)]. The elementary generators in \mathbb{H} and \mathbb{S} are indexed by a Pauli operator P and we denote them by $\{H_P\}$ and $\{S_P\}$, respectively. Elementary generators in the other two classes are indexed by distinct pairs (P, Q) of distinct Paulis [50] and denoted by $\{C_{P,Q}\}$ and $\{A_{P,Q}\}$, respectively. We can write any $L \in \mathbb{L}$ as a linear combination of elementary generators with real coefficients,

$$\begin{aligned} L &= L_{\mathbb{H}} + L_{\mathbb{S}} + L_{\mathbb{C}} + L_{\mathbb{A}} \quad (7) \\ &= \sum_P h_P H_P + \sum_P s_P S_P \\ &\quad + \sum_{P,Q>P} c_{P,Q} C_{P,Q} + \sum_{P,Q>P} a_{P,Q} A_{P,Q}. \quad (8) \end{aligned}$$

We refer to each coefficient as the *rate* of the corresponding error process, in keeping with its appearance in the exponent of $\mathcal{E} = e^L$.

A. Choi sums and units

The easiest way to define these elementary generators is using another commonly used representation that we call the *Choi-sum* representation [51,52]:

$$G[\cdot] = \sum_{P,Q \in \mathcal{P}} \chi_{P,Q} P \cdot Q. \quad (9)$$

There is a χ -matrix representation for every superoperator G . Equation 9 can be seen as an expansion of G in a complete orthogonal basis of superoperators that we call *Choi units*, defined by $X_{P,Q}[\cdot] = P \cdot Q$. It is easy to show that the Choi units are mutually orthogonal (by the Hilbert-Schmidt inner product defined on superoperators) and since there are $d^4 = 16^N$ of them, they form a complete basis. The Choi-sum representation can be defined with respect to any operator basis (a common choice is the basis of matrix units $\{|i\rangle\langle j|\}$) but we only use the Pauli basis here. The best-known property of the Choi-sum representation is that G is CP if and only if $\chi \geq 0$ [52].

We now define elementary generators, in three steps.

B. Hamiltonian generators

First, we consider unitary error processes $\mathcal{E}[\rho] = U\rho U^\dagger$. Their generators are well known; if $U = e^{-iJ}$, then $\mathcal{E}[\rho] = e^{H_J}[\rho]$, where $H_J[\rho] = -i[J, \rho]$. Since any Hamiltonian

J can be expanded in the Pauli basis as $J = \sum_P h_P P$, we can write $H_J = \sum_P h_P H_P$ and so the generator of any unitary error can be written as a linear combination of $d^2 - 1$ *Hamiltonian generators*:

$$H_P[\rho] = -i[P, \rho] = -iP\rho\mathbb{1} + i\mathbb{1}\rho P, \quad (10)$$

where the last expression is explicitly a Choi sum. \mathbb{H} is the $(d^2 - 1)$ -dimensional subspace of \mathbb{L} spanned by the Hamiltonian generators. It is invariant under unitary changes of basis—i.e., if $\mathcal{E} = e^{\sum_P h_P H_P}$, then for any unitary matrix U with superoperator representation $\mathcal{U}[\cdot] = U \cdot U^\dagger$, $\mathcal{U}\mathcal{E}\mathcal{U}^\dagger = e^{\sum_P h'_P H'_P}$ for some set of coefficients $\{h'_P\}$.

C. Stochastic generators

Second, we consider errors that are convex mixtures of unitaries. These are not generated by a linear combination of Hamiltonians, $J = \sum_k J_k$. Instead, the dynamical evolution of the system is a linear combination of the evolutions resulting from those J_k , i.e.,

$$\mathcal{E}[\rho] = \sum_k p_k e^{-iJ_k} \rho e^{iJ_k}, \quad \sum_k p_k = 1. \quad (11)$$

We treat the $\{J_k\}$ as small and expand in powers of them. To first order in $\{J_k\}$, the corresponding generator is indeed just $H_J = \sum_k p_k H_{J_k}$. But including second-order terms yields

$$\mathcal{E}[\rho] \approx \rho + H_J[\rho] + \sum_k p_k \left(J_k \rho J_k - \frac{1}{2} \{J_k^2, \rho\} \right). \quad (12)$$

Expanding each J_k in the Pauli basis and rearranging yields a sum of the form

$$\begin{aligned} \mathcal{E}[\rho] \approx & \rho + H_J[\rho] + \sum_P s_P (P\rho P - \rho) \\ & + \sum_{P,Q>P} c_{P,Q} \left(P\rho Q + Q\rho P - \frac{1}{2} \{P, Q\}, \rho \right), \quad (13) \end{aligned}$$

for some s_P and $c_{P,Q}$ coefficients that can be computed from the Pauli expansions of the J_k . So *any* convex mixture of small unitary evolutions is generated to leading order [53] by (1) the Hamiltonian generators discussed above plus (2) some linear combination of $d^2 - 1$ *stochastic Pauli generators* indexed by Pauli operators P ,

$$S_P[\rho] = P\rho P - \mathbb{1}\rho\mathbb{1}, \quad (14)$$

and $(d^2 - 1)(d^2 - 2)/2$ *Pauli-correlation generators* indexed by distinct pairs of nonidentity Paulis (P, Q) ,

$$C_{P,Q}[\rho] = P\rho Q + Q\rho P - \frac{1}{2} \{P, Q\}, \rho. \quad (15)$$

Equations (14) and (15) share a two-part structure. The first part is a symmetrized Choi unit, $P\rho P$ or $P\rho Q + Q\rho P$, that is unique to each distinct generator. The second part is a correction term, $-\mathbb{1}\rho\mathbb{1}$ or $-\{[P, Q]/2, \rho\}$, that is not unique to each elementary generator. All S generators share the same correction term, while the C generators can be divided into subfamilies indexed by $\{P, Q\}$. The purpose of the correction term is simple. It is necessary to ensure trace preservation. The S correction terms are easy to interpret: S generators *increase* the probability of the state $P\rho P$ and must therefore *reduce* the probability of $\rho = \mathbb{1}\rho\mathbb{1}$. The C correction terms are more obscure. They appear only when P and Q commute, and they cancel the state-dependent change in trace produced by $\rho \rightarrow P\rho Q + Q\rho P \implies \text{Tr}(\rho) \rightarrow \text{Tr}[(PQ + QP)\rho]$.

The \mathbb{S} and \mathbb{C} subspaces are spanned by the S and C generators, respectively. It is easy to show that each of these generators can be independently varied, just by considering mixtures of e^{iJ} and e^{-iJ} with $J \propto P$ or $J \propto P \pm Q$. The union of \mathbb{S} and \mathbb{C} is a $d^2(d^2 - 1)/2$ -dimensional subspace of stochastic generators. It is also invariant under unitary changes of basis.

D. Active (antisymmetric) generators

Third, we consider everything that is left. \mathbb{L} has $d^2(d^2 - 1)$ dimensions and we have constructed disjoint subspaces \mathbb{H} ($d^2 - 1$ dimensions), \mathbb{S} ($d^2 - 1$ dimensions), and \mathbb{C} [$(d^2 - 1)(d^2 - 2)/2$ dimensions]. Their complement, then, has $(d^2 - 1)(d^2 - 2)/2$ dimensions.

To construct elementary generators for this subspace, we consider how the H , S , and C elementary generators relate to the Choi units $X_{P,Q}$. The Choi units span the entire d^2 -dimensional space of superoperators, which is larger than \mathbb{L} because it contains non-TP processes. Each of the stochastic S and C generators is a linear combination of *symmetrized* Choi units—i.e., $X_{P,P}$ or $X_{P,Q} + X_{Q,P}$. The Hamiltonian H generators are antisymmetrized linear combinations proportional to $X_{P,\mathbb{1}} - X_{\mathbb{1},P}$. All of the H , S , and C generators are orthogonal to all the antisymmetrized Choi units of the form $X_{P,Q} - X_{Q,P}$ with $P, Q \neq \mathbb{1}$. Informed by this observation and by the fact that physical processes must be TP, we construct $(d^2 - 1)(d^2 - 2)/2$ additional error generators indexed by distinct pairs of nonidentity Paulis,

$$A_{P,Q}[\rho] = i \left(P\rho Q - Q\rho P + \frac{1}{2} \{[P, Q], \rho\} \right). \quad (16)$$

We call these *active generators* (see Sec. VH) but “antisymmetric” is equally appropriate (although Hamiltonian generators, which are also antisymmetric, are treated separately). Like the C and S generators, each A generator has a unique part $P\rho Q - Q\rho P$ and a correction term $i\{[P, Q]/2, \rho\}$ that is necessary to ensure TP. The A generators span the \mathbb{A} subspace of \mathbb{L} .

E. The dual basis

In Secs. VB–VD, we have constructed $d^2(d^2 - 1)$ linearly independent elementary error generators, in four classes, that partition the error generator space as $\mathbb{L} = \mathbb{H} \oplus \mathbb{S} \oplus \mathbb{C} \oplus \mathbb{A}$. Their collected actions, for easy reference, are as follows:

$$H_P[\rho] = -i[P, \rho] = -iP\rho\mathbb{1} + i\mathbb{1}\rho P, \quad (10)$$

$$S_P[\rho] = P\rho P - \mathbb{1}\rho\mathbb{1}, \quad (14)$$

$$C_{P,Q}[\rho] = P\rho Q + Q\rho P - \frac{1}{2} \{[P, Q], \rho\}, \quad (15)$$

$$A_{P,Q}[\rho] = i \left(P\rho Q - Q\rho P + \frac{1}{2} \{[P, Q], \rho\} \right). \quad (16)$$

These elementary error generators are not mutually orthogonal in the Hilbert-Schmidt inner product, but they have a very simple dual basis that can be used to extract the coefficient—or *rate*—of each elementary generator from an arbitrary error generator L :

$$H'_P[\cdot] = -\frac{i}{2d^2} [P, \cdot] = \frac{1}{d^2} H_P[\cdot], \quad (17)$$

$$S'_P[\cdot] = \frac{1}{d^2} P \cdot P, \quad (18)$$

$$C'_{P,Q}[\cdot] = \frac{1}{2d^2} (P \cdot Q + Q \cdot P), \quad (19)$$

$$A'_{P,Q}[\cdot] = \frac{i}{2d^2} (P \cdot Q - Q \cdot P). \quad (20)$$

These “dual elementary generators” are mutually orthogonal and simpler than the elementary generators constructed above. It is reasonable to ask why we did not use these definitions for the elementary generators themselves. The answer is that they are not TP. The elementary generators must be TP to ensure that they generate TP error channels. This can only be done by mixing in the special symmetric Choi units $X_{P,\mathbb{1}} + X_{\mathbb{1},P}$. But the dual generators do not have the same interpretation. They are not used to generate processes; their only role is in the extraction of the rates of elementary generators from arbitrary generators L as, for example,

$$h_P \equiv \text{Tr} \left(H'_P{}^\dagger L \right). \quad (21)$$

The dual generators do not need to be TP, and they are orthogonal to the special Choi units used to make the elementary generators TP.

We begin to explore the properties and nature of the H -, S -, C -, and A -type error generators by constructing them explicitly for one- and two-qubit systems as a concrete example.

F. One-qubit elementary error generators

An arbitrary one-qubit CPTP process G that is close to its target \bar{G} can be described by a 4×4 superoperator, written in the Pauli basis $(\mathbb{1}, X, Y, Z)$, the top row of which is fixed to ensure trace preservation [54]:

$$G = \begin{pmatrix} 1 & 0 & 0 & 0 \\ a & b & c & d \\ e & f & g & h \\ j & k & l & m \end{pmatrix} \bar{G}. \quad (22)$$

This error process has 12 free parameters, which map to 12 elementary error generators:

- Three Hamiltonian generators indexed by a Pauli P (H_X, H_Y, H_Z).
- Three Pauli-stochastic generators indexed by a Pauli P (S_X, S_Y, S_Z).
- Three Pauli-correlation generators indexed by nonequal pairs of Paulis P, Q ($C_{X,Y}, C_{Y,Z}, C_{X,Z}$).
- Three active generators indexed by nonequal pairs of Paulis P, Q ($A_{X,Y}, A_{Y,Z}, A_{X,Z}$).

Any single-qubit error generator L can be written as a linear combination of these generators [Eqs. (7)–(8)].

H_P terms generate unitary rotations of the Bloch sphere, which are coherent errors in the gate (see Fig. 3). The three coefficients (h_X, h_Y, h_Z) indicate the rate of erroneous rotation with respect to each Pauli axis. Together, they form a Bloch-sphere vector \vec{h} whose direction is the axis of the unitary rotation and whose length is its angle [55]. If an error is purely coherent, then its error generator will be restricted to the \mathbb{H} subspace.

S_P terms shrink the Bloch sphere to an ellipsoid aligned with the X, Y , and Z axes (see Fig. 4). Each S_P generates dephasing toward the P axis—e.g., S_Z shrinks polarization along the X and Y axes, but leaves Z alone. The three S_P generators generate Pauli channels, which appear in quantum error correction theory [24,56–62] and quantum process characterization [63,64].

Dephasing along other axes in the Bloch sphere is also possible. It is generated by combinations of the S_P and the Pauli-correlation $C_{P,Q}$ generators. By themselves, the three $C_{P,Q}$ generators are never physically valid (they generate non-CP maps). They generate zero-determinant “squeezing” of the Bloch sphere, causing it to shrink and grow along perpendicular axes. For example, the $C_{X,Z}$ generator acts (see Fig. 5) as

$$\begin{aligned} C_{X,Z}[X + Z] &= X + Z, \\ C_{X,Z}[X - Z] &= -(X - Z), \\ C_{X,Z}[Y] &= C_{X,Z}[\mathbb{1}] = 0, \end{aligned}$$

so it “inflates” the $X + Z$ axis of the Bloch sphere and shrinks the $X - Z$ axis. But adding it to $S_X + S_Z$ yields

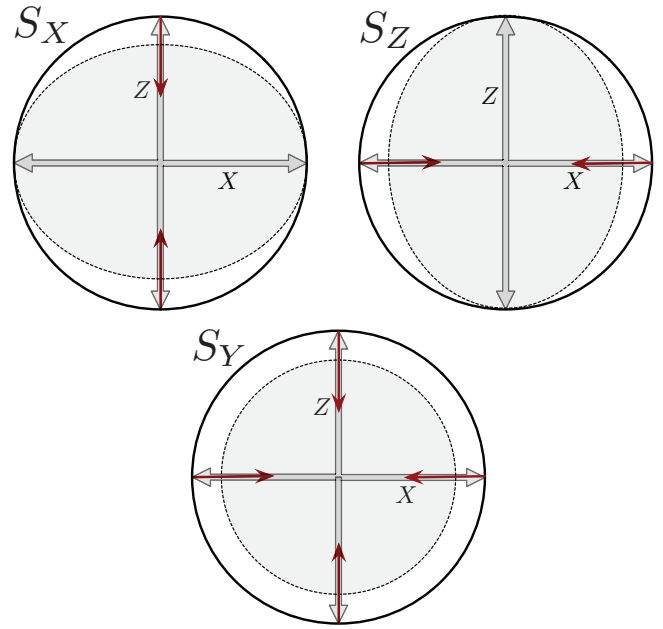


FIG. 4. The action of one-qubit Pauli-stochastic error generators on the X - Z plane of the Bloch sphere. S_X shrinks $Z \rightarrow 0$ but leaves X unchanged. S_Z shrinks $X \rightarrow 0$ but leaves Z unchanged. S_Y shrinks both X and Z . Each generator, by itself, generates a dephasing process. The sum of all three generates depolarization.

a generator of $X + Z$ errors that preserves $X + Z$ and shrinks $X - Z$, dephasing the Bloch sphere toward the $X + Z$ axis (see Fig. 6).

Unlike the Hamiltonian rates (h_X, h_Y, h_Z) , which form a Bloch sphere vector, the stochastic rates form a symmetric tensor in the same space,

$$\Sigma = \begin{pmatrix} s_X & c_{X,Y} & c_{X,Z} \\ c_{X,Y} & s_Y & c_{Y,Z} \\ c_{X,Z} & c_{Y,Z} & s_Z \end{pmatrix}, \quad (23)$$

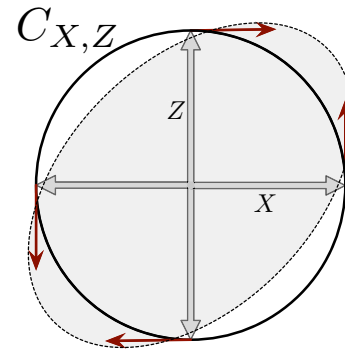


FIG. 5. The action of a representative Pauli-correlation error generator. This is how the one-qubit $C_{X,Z}$ generator acts on the X - Z plane of the Bloch sphere. Its action on Z is identical to that of H_Y , taking $Z \rightarrow X$, but instead of taking $X \rightarrow -Z$, it takes $X \rightarrow Z$. The result is a squeezing transformation that stretches the $X + Z$ axis and shrinks the $X - Z$ axis.

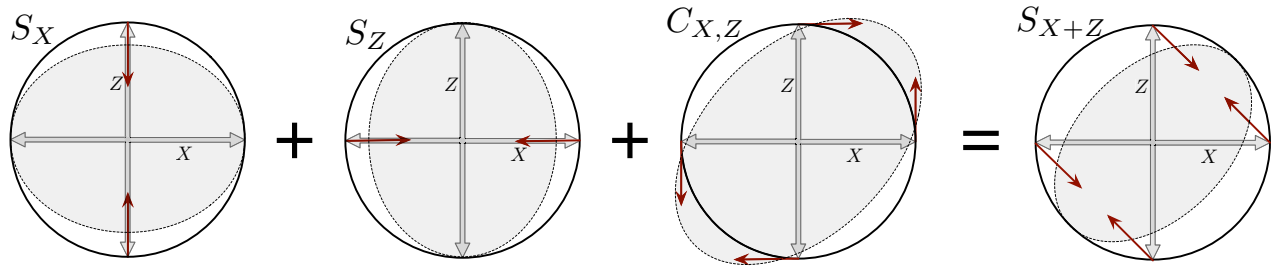


FIG. 6. Pauli-correlation generators are “modifiers” that combine with stochastic generators to generate non-Pauli-stochastic errors. As shown here, the sum $S_X + S_Z + C_{X,Z}$ generates a CPTP stochastic error process (dephasing) along the $X + Z$ axis.

which describes an error process that shrinks the Bloch sphere to an ellipsoid.

The three $A_{P,Q}$ generators, called “active” or “antisymmetric” in Sec. V D, can also be called “affine” generators for a single qubit, because they generate affine shifts of the Bloch sphere. For example, $A_{X,Y}$ acts (see Fig. 7) as

$$\begin{aligned} A_{X,Y}[\mathbb{1}] &= -4Z, \\ A_{X,Y}[X] &= A_{X,Y}[Y] = A_{X,Y}[Z] = 0. \end{aligned}$$

So for *any* density matrix ρ , $A_{X,Y}[\rho] = -2Z$. Similarly, $A_{X,Z}$ and $A_{Y,Z}$ generate affine shifts in the Y and X directions, respectively. Like the C -type generators, these are never physically valid by themselves. But when combined with S -type generators, they produce nonunital decoherence processes. The best-known example is T_1 decay, aka amplitude damping from $|1\rangle$ to $|0\rangle$, given by

$$\Gamma_{1 \rightarrow 0}[\rho] = \gamma \sigma_- \rho \sigma_-^\dagger + \sigma_0 \rho \sigma_0^\dagger, \quad (24)$$

where $\sigma_- = |0\rangle\langle 1|$ and $\sigma_0 = (|0\rangle\langle 0| + \sqrt{1-\gamma}|1\rangle\langle 1|)$. Amplitude damping shrinks the Bloch sphere to a Pauli-aligned ellipsoid (like a combination of Pauli-stochastic

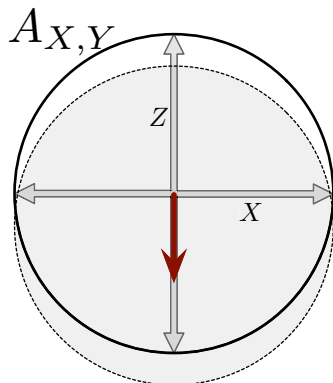


FIG. 7. The action of a representative active error generator. This is how the one-qubit $A_{X,Y}$ generator acts on the X - Z plane of the Bloch sphere. It has no action at all on the X , Y , or Z operators, but it sends $\mathbb{1} \rightarrow -4Z$. It thus shifts the entire Bloch sphere downward.

errors) but also shifts it affinely in the Z direction. Its generator (see Fig. 8) is proportional to

$$S_X + S_Y + A_{X,Y}. \quad (25)$$

The process given in Eq. (24) is often treated as a wholly independent kind of error, distinct from stochastic Pauli errors. It is reasonable to ask why we represent it as a combination of stochastic Pauli errors and a non-CP affine shift, rather than as an independent elementary error generator. The answer is simple: there are *too many* processes like the one given in Eq. (24).

Given any point on the Bloch sphere, a process can be constructed that “damps” toward it [65]. But our goal here is to construct a set of linearly independent generators, so that any L can be uniquely decomposed as a linear combination of them. Those “damping” processes cannot all be linearly independent. But if we consider them in the context of the S and C generators already constructed, then the A generators precisely span the additional degrees of freedom contributed by “damping” processes. For example, the $A_{X,Y}$ generator is a *difference* of amplitude-damping processes,

$$A_{X,Y} \propto \Gamma_{1 \rightarrow 0} - \Gamma_{0 \rightarrow 1}. \quad (26)$$

The $A_{X,Z}$ and $A_{Y,Z}$ affine generators can be defined similarly in terms of amplitude-damping processes in the Y and X bases, respectively. Their coefficients $(a_{y,z}, a_{x,z}, a_{x,y})$ form a Bloch-sphere vector that indicates the direction in which the maximally mixed state will be shifted by the \mathbb{A} portion of the error generator.

G. Elementary error generators for two qubits

Many features and interpretations from the one-qubit example carry over to a two-qubit system. However, there are a few novelties that make it worth examining.

If we consider a two-qubit process G and its error generator L (Fig. 2), they both have $256 - 16 = 240$ free parameters. We can identify and construct Hamiltonian and Pauli-stochastic generators (15 each, indexed by the 15 nontrivial two-qubit Pauli operators) exactly as for one qubit.

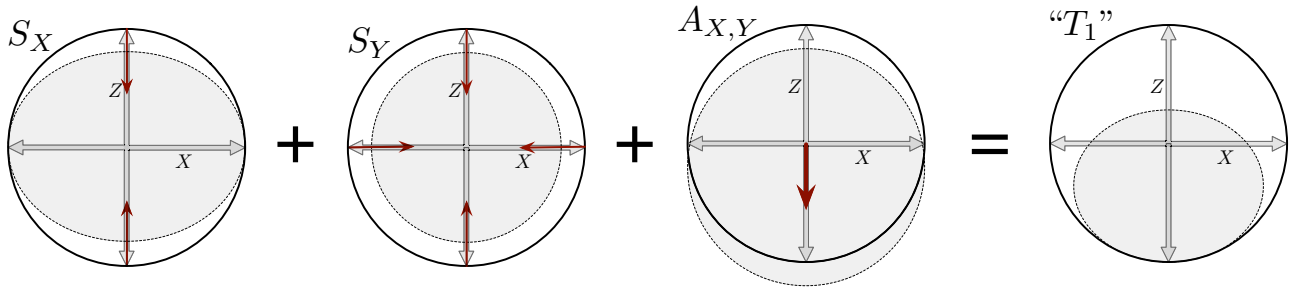


FIG. 8. Like Pauli-correlation (C) generators, active generators are “modifiers” that combine with stochastic generators to generate more familiar processes. As shown here, the sum $S_X + S_Y + A_{X,Y}$ generates a nonunital amplitude-damping or “ T_1 ” process that describes cooling or dissipative decay toward the $|0\rangle\langle 0|$ state.

There are 105 linearly independent two-qubit Pauli-correlation generators. A new phenomenon appears for two qubits, because $P\rho Q + Q\rho P$ is only TP if P and Q anticommute. In the one-qubit example, every pair of distinct traceless Pauli operators anticommutes. But in a two-qubit system, there are also pairs such as $(\mathbb{1}Z, ZZ)$ that commute. For these cases, the double anticommutator term in the definition of $C_{P,Q}$ [Eq. (15)] becomes nonzero and ensures that the generator is TP. This term has some odd consequences, discussed in Sec. VII.

The A -type generators hold more surprises. For one qubit, there are exactly three A -type generators. They all generate pure affine shifts (e.g., $A_{X,Y}[\rho] = -2Z$) and their rates conveniently form a vector in Hilbert-Schmidt space. But for a two-qubit system, there are 105 A -type generators and they do not generally produce affine shifts in any particular direction.

To understand their action, we start by considering $A_{P,Q}$ when P and Q both act nontrivially only on one (the same) qubit—e.g., $A_{X\mathbb{1},Y\mathbb{1}}$. This elementary generator can also be written as $A_{X,Y} \otimes \mathbb{1}$. It generates an affine shift on qubit 1 independent of the state of qubit 2:

$$A_{X\mathbb{1},Y\mathbb{1}}[\rho_1 \otimes \rho_2] = -2Z \otimes \rho_2, \quad (27)$$

$$A_{X\mathbb{1},Y\mathbb{1}}[\rho_{12}] = -2Z \otimes \text{Tr}_1(\rho_{12}). \quad (28)$$

It naturally appears as part of the generator for a local amplitude damping process $\Gamma_{1 \rightarrow 0} \otimes \mathbb{1}$ that acts only on qubit 1.

This example can be generalized. It involves two anti-commuting Paulis acting on one qubit. But any two anti-commuting Paulis generate a one-qubit Pauli algebra and can be viewed as the effective “ X ” and “ Y ” operators for a virtual qubit encoded somewhere within the two-qubit Hilbert space. So, every $A_{P,Q}$ where $\{P, Q\} = 0$ induces an affine shift in the direction of $i[P, Q]$ on *some* virtual one-qubit subsystem. For example, both $A_{X\mathbb{1},Y\mathbb{1}}$ and $A_{XX,YX}$ induce affine shifts in the $Z\mathbb{1}$ direction but they do so acting on different one-qubit subsystems.

There are also A -type generators that produce no affine shift at all. One such example is a difference of two A -type

generators that produce the same affine shift, e.g., $A_{X\mathbb{1},Y\mathbb{1}} - A_{XX,YX}$. A more fundamental example, though, is given by the $A_{P,Q}$ generators for *commuting* pairs of Paulis. Here, $[P, Q] = 0$, and $A_{P,Q}[\rho] = i(P\rho Q - Q\rho P)$, so $A_{P,Q}[\mathbb{1}] = 0$. No affine shift occurs—the generated process is unital.

We do not have a clear or intuitive understanding of these generators and when (if ever) they are likely to have significant rates in realistic quantum processors. However, we discuss their action and the rationale for calling them “active” in the next section.

H. Discussion

A taxonomy is a classification of things or concepts. So far, we have shown *how* to represent the small Markovian error in a gate g as an error generator L and how to decompose L in a basis of elementary error generators. We now return to the implicit promise of the title and present a taxonomy of small Markovian errors that classifies them into sensible categories. Most of this analysis is implicit in the preceding sections, so our goal here is to make it explicit and fill in the gaps.

We cannot classify an arbitrary L as representing one kind of error *or* another, because it will be a linear combination of all the elementary generators listed above. Instead, L represents a *mixture* of different sorts of errors. The elementary generators constitute a classification of the phenomena that can be mixed together to make an arbitrary error L . So in analyzing such an L , the taxonomy enables separating those components out to make statements such as “The error in g is primarily Hamiltonian (coherent),” or “The error in g is 35% Hamiltonian and 65% stochastic, and the stochastic error is almost all Pauli stochastic,” or “The rate of single-qubit Hamiltonian errors in g is 1.7%.” We seek to complete the project that Kueng *et al.* [66] initiated by classifying single-qubit error modes and their impact.

The root of the taxonomy that we propose is the partition of error-generator space (\mathbb{L}) into Hamiltonian (\mathbb{H}), stochastic ($\mathbb{S} \oplus \mathbb{C}$), and active (\mathbb{A}) subspaces. These subspaces are unitarily invariant, which means that the

classification of a particular error as “Hamiltonian,” “stochastic,” or “active” is unaffected by time evolution, change of basis, or whether the generator comes before or after (or during) a unitary target gate. So, given an arbitrary L , it is meaningful to separate it into its components on distinct sectors, $L = L_{\mathbb{H}} + (L_{\mathbb{S}} + L_{\mathbb{C}}) + L_{\mathbb{A}}$, and consider each term (more or less) independently. As belied by our notation, we often find it useful to subdivide the stochastic sector into Pauli-stochastic and Pauli-correlation sectors. This division is less fundamental, as we discuss below.

Hamiltonian errors are widely well understood and require little discussion. Any $L_{\mathbb{H}}$ whatsoever generates a legitimate and physically valid unitary error process, often called a *coherent error*. Coherent errors can be eliminated, in principle, by dynamical decoupling or recalibrating control. Variations of $L_{\mathbb{H}}$ are completely independent of errors on the other sectors—e.g., changing $L_{\mathbb{H}}$ does not affect the complete positivity or the interpretation of any other error generators.

Stochastic errors are unital (they preserve the maximally mixed state) and produce no net rotation of the state space. They were introduced in Sec. VB as the nonunitary consequences of small *random unitary* dynamics—i.e., mixtures of different unitary rotations [67]. But like most quantum processes, stochastic errors can have multiple distinct physical causes [68]. Stochastic errors can also be produced by *minimally disturbing measurements* [69]. For example, if the environment of a qubit measures it weakly in the Z basis, the qubit will experience dephasing, which is a stochastic Z error. More generally, discarding the outcome of any minimally disturbing measurement produces a quantum process

$$\mathcal{E}[\rho] = \sum_k M_k \rho M_k, \quad (29)$$

where each $M_k \geq 0$ and $\sum_k M_k^2 = \mathbb{1}$. Positivity implies that each M_k is Hermitian and can be expanded as a sum of Paulis with strictly real coefficients. This means that the error process in Eq. (29) has a strictly symmetric Choi-sum form, so it is orthogonal to all H - and A -type generators and thus wholly stochastic.

There is no compelling *mathematical* reason to separate the \mathbb{S} and \mathbb{C} generators. As observed earlier, their rates are the diagonal and off-diagonal components of a symmetric tensor and so unitary changes of basis will mix them. But separating them makes *practical* sense, because the Pauli basis is very special in quantum information science. Experimental gates are often generated by Pauli Hamiltonians. Stochastic Pauli error rates appear throughout the theory of quantum error correction [24,56–64]. And the Clifford group—the automorphism group of the Paulis—appears frequently in both experimental gate sets and theoretical constructions [24,70–73]. Although unitary transformations do not generally preserve the \mathbb{S} - \mathbb{C}

separation, Clifford transformations do. So, in an experimental or theoretical context that privileges the Pauli or Clifford operations, this separation is likely to be useful. In others, it may not.

There are two key distinctions between the S and C generators. First, any linear combination of S generators yields a physically valid process if (and almost [74] only if) the s_P rates are all non-negative. In contrast, the rate of each $C_{P,Q}$ can be either positive or negative but it is strictly bounded by the rates of S_P and S_Q . The constraint is nontrivial but easy to state: the symmetric matrix with diagonal elements S_P and off-diagonal elements $C_{P,Q}$ must be positive semidefinite. A simple consequence is that $|C_{P,Q}| \leq \sqrt{S_P S_Q}$. This has useful sparsity implications for estimating error processes: if only n of the $d^2 - 1$ Pauli-stochastic error rates are non-negligible, then all but $n(n - 1)/2$ Pauli-correlation rates can also be neglected.

Second, while S generators *cause* errors—i.e., their rates really are “error rates” of bit- or phase-flip errors— C generators only *modify* them. For example, if a qubit has $s_X = s_Z = 0.01$, then the total rate of bit- and phase-flip errors is 0.02. Varying the $c_{X,Z}$ coefficient over its entire range does not change this. It merely shifts the error mechanism from pure dephasing in the $X - Z$ basis, to independent bit- and phase-flip errors, to pure dephasing in the $X + Z$ basis.

It is tempting to imagine all stochastic errors as being unitarily equivalent to some Pauli channel. This would imply that the effect of the C generators is mainly to change the basis of the stochastic errors, which is precisely what they do in the special case of a single qubit. But for more than one qubit, this is not true. Consider the experimentally relevant example of a two-qubit controlled- Z gate (U_{CZ}) generated by the Hamiltonian $H \propto (\mathbb{1} + Z) \otimes Z$. Random fluctuations in the strength of the Hamiltonian will produce random over- and under-rotations that average to a stochastic controlled- Z error—i.e., a mixture of $\mathbb{1}$ and U_{CZ} itself. But U_{CZ} has eigenvalues $(1, 1, 1, -1)$, so this is *not* unitarily equivalent to a Pauli channel. The error generators for this error channel are S_{ZZ} , $S_{\mathbb{1}Z}$, and $C_{ZZ,\mathbb{1}Z}$. The $C_{ZZ,\mathbb{1}Z}$ generator changes spectral properties of the noise channel. This is a significant and meaningful change—it leaves the *average* probability of an error (over all input states) unchanged but concentrates it onto certain states ($|1\rangle \otimes |\psi\rangle$) rather than others ($|0\rangle \otimes |\psi\rangle$).

As observed above, C generators do not always generate physically valid processes. They are only valid if mixed with S generators in sufficient proportion. This is awkward. It would be far more satisfying to have an error generator basis in which *every* positive linear combination was physically valid. Sadly (but for interesting reasons), this is not possible.

It is forbidden by the geometry of the convex set of CPTP maps in the neighborhood of the identity. The identity channel is an extreme point of this set and resembles the pointy tip at the bottom of an ice-cream cone. Our

goal in this paper is to construct a complete, discrete basis of elementary error generators, of which any Lindbladian is a linear combination. Given any such basis, the set of all *positive* linear combinations of basis elements defines a polyhedral cone (e.g., an orthant, possibly stretched linearly). However, the set of CPTP maps in the neighborhood of the identity is a nonpolyhedral cone—it has “round” cross sections. These features stem from the positivity constraint on CPTP maps, which reflects the positive semidefinite constraint on density matrices that defines a Bloch sphere for qubit states instead of a “Bloch cube.” This nonpolyhedral cone cannot be generated by positive linear combinations of *any* discrete set of vectors.

So, the desirable goal of constructing a discrete spanning set of error generators, each of which generates unconditionally valid (CP) processes, is forbidden by the geometry of the CPTP set, which stems simply from the shape of the CPTP constraint. The S generators are a largest-possible set [75]—they are not a unique choice, but no larger set of linearly independent elementary error generators generates unconditionally valid processes. The same reasoning applies to the A generators discussed below.

Active (A-type) errors are relatively mysterious. We do not understand them to the same degree as Hamiltonian or stochastic errors. The effects that they produce appear rarely in theoretical models of quantum errors—with the sole major exception of T_1 (amplitude-damping) processes. Amplitude damping is nonunitary (it can decrease entropy) and only A -type error generators produce nonunitary error processes.

But T_1 decay, in quantum computing, is usually a single-qubit effect. It is a cooling process, where weak coupling between the dominant system Hamiltonian and a large cold environmental bath produces irreversible decay into lower-energy states. Gate-model quantum processors are usually designed with steady-state Hamiltonians that do not couple the qubits and transient controllable coupling Hamiltonians whose duration is too short to make qubits cool into correlated ground states. Independent T_1 decay on isolated qubits can be modeled entirely using just the weight-1 $A_{P,Q}$ generators where P and Q act trivially on all but one qubit. It is natural to ask what all the other A generators do.

Part of the answer is that multiqubit systems can have complicated Hamiltonians and experience complicated cooling processes. For example, additional A -type generators are required to model “ T_1 ” decay for a two-qubit system with a single ground state and a triply degenerate state. But the $A_{P,Q}$ generators for *commuting* (P, Q) are not nonunitary at all, so they have no direct relationship to cooling. These generators are entirely antisymmetric. Like Hamiltonian generators, they generate orthogonal $SO(d^2 - 1)$ rotations that rotate ρ in $L(\mathcal{H})$ without changing $\text{Tr}\rho^2$. But these rotations do *not* correspond to

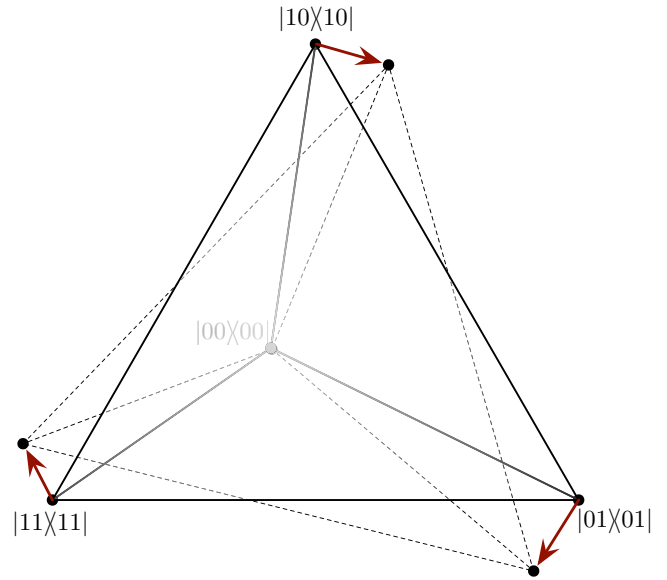


FIG. 9. A -type generators, by themselves, are always non-CP. Some of them generate affine shifts on one-qubit virtual subsystems but, in general, A -type generators cause orthogonal $SO(d^2 - 1)$ rotations on the space of density matrices that do *not* correspond to unitary $U(d)$ transformations on Hilbert space. A two-qubit example, shown here, is a rotation entirely within the space spanned by the projectors onto the four computational-basis states—or, equivalently, by $\{\mathbb{1}\mathbb{1}, \mathbb{1}Z, Z\mathbb{1}, ZZ\}$. The convex hull of the four computational basis states defines a classical simplex that is a cross section of the quantum state space. This $SO(4) \subset SO(15)$ rotation is generated by a linear combination of A -type generators and it maps the vertices of the simplex to points outside the simplex, which are not positive semidefinite density matrices.

unitaries and are therefore not CP by themselves (see Fig. 9).

The most general statement we can make about the A -type generators is that they are all produced by some form of *active feedback* from the environment [76]. Any quantum process can be written using a diagonalized Choi-sum form known as the *Kraus representation* [77],

$$\mathcal{E}[\rho] = \sum_k K_k \rho K_k^\dagger, \quad (30)$$

subject only to the constraint $\sum_k K_k^\dagger K_k = \mathbb{1}$. If we use the polar decomposition to write each $K_k = U_k M_k$, where U_k is unitary and M_k is positive semidefinite, then it is clear that \mathcal{E} can be implemented by (1) performing a minimally disturbing measurement described by the positive operator-valued measure $\{M_k^2\}$, (2) applying U_k *conditional* on the observed result, and (3) discarding the observed outcome k . If $U_k = \mathbb{1}$ for all k , then the process results from a minimally disturbing measurement. As shown in Sec. V C, such processes are entirely modeled by stochastic error

generators. If $U_k = \text{constant}$ regardless of k , then the process is the composition of (1) a minimally disturbing measurement and (2) a unitary. This corresponds to a combination of Hamiltonian and stochastic errors. It follows that A -type error generators are uniquely associated with error processes where U_k depends on k . This constitutes active feedback; the environment induces system dynamics *conditional* on the result of a measurement on the system.

Cooling (aka T_1 or amplitude-damping) is a special and well-understood example of active feedback. A T_1 process can be written explicitly as a one-sided weak measurement of Z , $\{p|1\rangle\langle 1|, \mathbb{1} - p|1\rangle\langle 1|\}$, followed by a bit-flip (X) operation conditional on observing the excited state $|1\rangle$. But active feedback can produce many other dynamics too. If we make $\{M_k^2\}$ a weak version of an informationally complete POVM, then by choosing the conditional unitaries U_k , we can produce a component of literally *any* orthogonal rotation in $SO(d^2 - 1)$.

In this construction, the orthogonal rotation generated by the A generators will be accompanied by a significant amount of stochastic error (S generators), which is caused by the measurement and not eliminated by the conditional unitary (see Fig. 10—and also Fig. 8 in retrospect). This illustrates that, like the Pauli-correlation generators, A -type generators are “modifiers.” They are never completely positive by themselves. The rate of $A_{P,Q}$ can have either sign but cannot be nonzero unless the corresponding S_P and S_Q error rates are both nonzero and $|a_{P,Q}| \leq \sqrt{s_P s_Q}$. Their main role is not to *create* errors but to move their impact around. The single-qubit T_1 process provides

a good example of this. Recall that it is generated by $S_X + S_Y + A_{X,Y}$. The stochastic error process generated by $S_X + S_Y$ alone flips both the $|0\rangle$ and $|1\rangle$ states with equal probability p . The T_1 process, on the other hand, never flips the $|0\rangle$ state but flips the $|1\rangle$ state with probability $2p$. This difference can be significant—for example, transmon-based processors perform better when ancilla qubits are stored in the $|0\rangle$ state, because of precisely this effect—but it does not change the *average* error rate of the gate.

VI. RELATIONSHIP TO LINDBLAD MASTER EQUATIONS

An error generator L was defined in Eq. (6) as the logarithm of an error process \mathcal{E} that is close to the identity process. This is very similar to—but not quite the same as—the generator of a Lindblad master equation [45], known as a *Lindbladian*.

The most familiar and common form of the Lindblad master equation is probably

$$\dot{\rho} = -\frac{i}{\hbar}[H, \rho] + \sum_{i=1}^{d^2-1} \gamma_i \left(L_i \rho L_i^\dagger - \frac{1}{2} \{L_i^\dagger L_i, \rho\} \right). \quad (31)$$

But this rather complicated expression hides a great simplicity. We can write the Lindblad master equation much more simply, as

$$\dot{\rho} = L_+[\rho], \quad (32)$$

where L_+ is a superoperator required to satisfy a simple condition: L_+ is a valid Lindbladian if and only if e^{tL_+} is a CPTP map for all $t > 0$. It is sufficient for e^{tL_+} to be CPTP for arbitrarily small $t \rightarrow 0_+$, where $e^{tL_+} \rightarrow \mathbb{1} + tL_+$, so the sole purpose of all the structure on the right-hand side of Eq. (31) is to ensure that $\mathbb{1} + tL_+$ is both CP and TP for arbitrarily small t .

For every Lindbladian L_+ , there is a corresponding error process $\mathcal{E} = e^{L_+}$. But the reverse does not hold: there are error processes \mathcal{E} for which $L = \log \mathcal{E}$ is not a Lindbladian. These processes are said to not be *infinitely divisible* [78] and are sometimes called *non-Markovian* (see, e.g., Ref. [79]). This nomenclature appears to conflict with our assertion that *any* CPTP map describes Markovian dynamics.

The root cause of the confusion is the distinction between continuous-time dynamics and discrete-time dynamics. A process has the Markov property if (and only if) its state at time $t' > t$ is determined entirely by the state at time t (and the nature of the process, of course). It is necessary to state what values t may take. In contexts where t takes ordinal values (e.g., $t = 0, 1, 2, \dots$), time is discrete; when t is allowed to take real values, time is continuous.

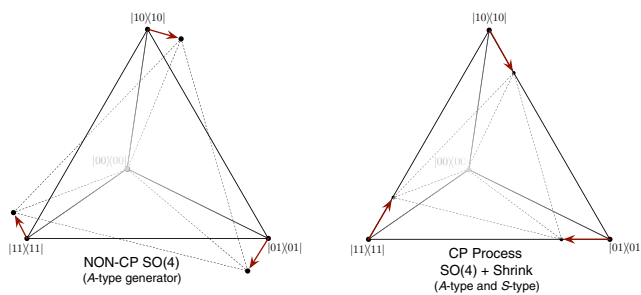


FIG. 10. When maps generated by A -type generators are implemented via nonminimally disturbing measurements (measurement followed by a conditional unitary), they are accompanied by S -type decoherence that shrinks the state space enough to ensure complete positivity. Here, this is shown for the example of Fig. 9. The illustration on the left shows the action of a non-CP process generated by *only* A -type generators on the computational-basis simplex. The illustration on the right shows the action of a CPTP process with the same A -type generators but additional S -type generators that are inevitable consequences of the measurement. The T_1 process in Fig. 8 can be seen as an example of exactly the same phenomenon but with an A -type generator that produces an affine shift.

So, *any* quantum process (CPTP map) \mathcal{E} can define a discrete-time Markov semigroup,

$$\{\mathbb{1}, \mathcal{E}, \mathcal{E}^2, \mathcal{E}^3, \dots\}. \quad (33)$$

But it is reasonable to go further and ask whether this discrete semigroup can be embedded in a continuous-time semigroup $\{e^{t \log \mathcal{E}}\}$. This is equivalent to asking whether \mathcal{E} could have been *caused* by continuous-time Markovian dynamics. In contrast, the discrete-time semigroup describes the discrete-time Markovian dynamics that *results* from \mathcal{E} . Both are interesting and useful concepts. But the continuous-time paradigm is more relevant to understanding the causes and mechanisms of error within a gate, while the discrete-time paradigm is more relevant to understanding the computational consequences of those errors. (A pithy summary might be “Physics clocks are continuous; computer clocks are discrete.”)

In this paper, we are not intrinsically concerned with the divisibility of \mathcal{E} . In fact, we explicitly avoid any inference about how G is generated (see Sec. IV), because quantum logic gates are *always* induced by time-varying processes and so we do not generally expect them to be consistent with Markovian continuous-time dynamics. But this does not provide license to ignore divisibility, because if \mathcal{E} is *not* infinitely divisible, then its logarithm L is not a Lindbladian. This has consequences. Our goal in this section is to discuss, bound, and mitigate those consequences.

If $L = \log \mathcal{E}$ is not Lindbladian, then there exists *some* t for which e^{tL} is not CP. Since $\mathcal{E} = e^L$ is CP, violations of CP can never be observed at integer t and the largest violation will occur for $t \in (0, 1)$ [80]. We do not propose to construct such maps; our goal is to describe errors in G and to compute their consequences when a discrete (integer) number of gates are applied in sequence. Within this context, we will never observe violations of CP directly.

What we *do* need to deal with, however, are the analytic consequences of L not (necessarily) being a Lindbladian. These consequences are mitigated by our restriction to *small* errors—i.e., to $\mathcal{E} \approx \mathbb{1}$. Indivisible maps can be found arbitrarily close to $\mathbb{1}$, so small errors do not eliminate the issue. A useful example of an indivisible map close to $\mathbb{1}$ is the process that acts as

$$\mathcal{E}[\rho] = (1 - 2p)\rho + pX\rho X + pY\rho Y. \quad (34)$$

A Lindblad generator for this process would need to independently generate X and Y errors at rate p . But such a generator would produce an X error *and* a Y error with probability p^2 , and this effects a Z error. No continuous-time Markovian process can cause both X and Y errors without also causing Z errors. If we compute $\log \mathcal{E}$ for Eq. (34), we get an $O(p^2)$ *negative* rate of Z errors, which makes the net probability of a Z error equal to zero at $t = 1$ but makes $e^{t \log \mathcal{E}}$ non-CP for $t \in (0, 1)$.

Restricting to small errors mitigates this issue because, although L is not always a Lindbladian, it is very *close* to a Lindbladian when the error is small. More precisely: if $L = \log \mathcal{E}$, then there exists a valid Lindbladian L' such that $L' - L = O(L^2)$. To show this, it is sufficient to choose $L' = \mathcal{E} - \mathbb{1}$. This is a valid Lindbladian (Lemma 1 of [81]), and its closeness to L follows from the series expansion $\log(\mathcal{E}) = (\mathcal{E} - \mathbb{1}) - \frac{1}{2}(\mathcal{E} - \mathbb{1})^2 + o[(\mathcal{E} - \mathbb{1})^2]$. A useful corollary is that although $\mathcal{E} \approx \mathbb{1}$ may not be divisible, there always exists a nearby divisible \mathcal{E}' with $|\mathcal{E}' - \mathcal{E}| = O(|\mathcal{E} - \mathbb{1}|^2)$.

These two observations provide two ways to use L as “almost” a Lindbladian. First, we can take the logarithm of any small \mathcal{E} and treat it as a Lindbladian, at the price of accepting small $O(L^2)$ violations of positivity. Second, we can treat L as the fundamental thing, restrict it to be a valid Lindbladian, and be confident that we can approximate any \mathcal{E} to within $O(|\mathcal{E} - \mathbb{1}|^2)$ by $\mathcal{E} \approx e^L$.

We could have avoided nonpositivity entirely by simply defining L differently, as $L = L^\Delta \equiv \mathcal{E} - \mathbb{1}$ in Sec. IV. This is still a valid choice—none of the subsequent analysis (e.g., elementary error generators) would be different, and the rates of various errors would only change at $O(|L^2|)$. A clean example of how this would change error rates can be obtained by considering two slightly different versions of the example given in Eq. (34):

$$\mathcal{E}_a = \rho \rightarrow (1 - 2p)\rho + pX\rho X + pY\rho Y, \quad (35)$$

$$\mathcal{E}_b = \exp(pS_X + pS_Y). \quad (36)$$

Both are CPTP. The first is indivisible; the second is continuous-time Markovian. If we compute error generators using the logarithm, we obtain

$$L_a = pS_X + pS_Y - p^2S_Z + o(p^2), \quad (37)$$

$$L_b = pS_X + pS_Y. \quad (38)$$

If we compute them using the difference, we obtain

$$L_a^\Delta = pS_X + pS_Y, \quad (39)$$

$$L_b^\Delta = pS_X + pS_Y + p^2S_Z + o(p^2). \quad (40)$$

In our experience, the first representation is more informative—nondivisible error processes are flagged by negative error rates and the rates of rare error processes (e.g., correlated errors) are not contaminated by quotidian collisions between two common error processes. But we believe that which choice is “better” remains, at the least, an open question. It is possible, as experimental resolution into error processes increases, that both conventions will find specific practical applications.

VII. SIMPLE ERROR METRICS

We have shown how to take the process matrix for an imperfect gate, transform it to a list (or vector) of error

rates, partition those rates into distinct classes (subspaces), and interpret each one. But that list of error rates can still be very long. Often, it is desirable to condense a detailed description of the error process into one or two summary statistics. Several error metrics exist for process matrices [82], of which the most commonly used (in recent years) are *process fidelity* (with the target gate) and *diamond norm error* (distance to the target gate).

Describing imperfect gates by their error generators does not preclude use of existing metrics. An error generator is a faithful description of the process matrix, so it is easy to reconstruct $G = e^{L\overline{G}}$ and compute its fidelity with, or diamond norm distance to, \overline{G} . But error generators provide the opportunity to consider alternative metrics that may be more natural in the limit of small errors. Here, we introduce two such metrics, briefly discuss their suitability for small errors represented by generators, and sketch their relationship to well-known metrics including fidelity and diamond norm. This is *not* intended as a comprehensive investigation of the subject.

Both metrics are based on the *Jamiolkowski state* of a process [83]. It is linearly isomorphic to the χ matrix and is given by

$$\rho_J(\mathcal{E}) = (\mathcal{E} \otimes \mathbb{1}) [|\Psi\rangle\langle\Psi|], \quad (41)$$

where $|\Psi\rangle$ is a maximally entangled state between the system of interest and an auxiliary system of the same dimension. We want metrics for error *generators*. These are not processes; they are infinitesimal generators of processes. The Jamiolkowski “state” for a generator L is defined by substituting $\mathcal{E} \rightarrow L$ into the formula [Eq. (41)] for ρ_J , but it is not actually a density matrix. Instead, it is proportional to a *difference* between density matrices.

A. Jamiolkowski probability

We call the first metric *Jamiolkowski probability* (or “J-probability” for short). It is the total probability created by L on the orthogonal complement to $|\Psi\rangle$ (see Fig. 11):

$$\epsilon_J(L) = \text{Tr}[\rho_J(L) (\mathbb{1} - |\Psi\rangle\langle\Psi|)] \quad (42)$$

$$= -\text{Tr}[\rho_J(L) |\Psi\rangle\langle\Psi|]. \quad (43)$$

It is extremely simple to compute the J-probability for each elementary generator: $\epsilon_J = 1$ for every S_P generator and $\epsilon_J = 0$ for every other elementary generator. If an error generator L is represented by the list of rates $\{h_P, s_P, c_{P,Q}, a_{P,Q}\}$, then $\epsilon_J(L) = \sum_P s_P$.

The J-probability of a generator quantifies the average rate at which it “flips” a state to some orthogonal state. Geometrically, it measures shifts in ρ that commute with ρ and thus change the spectrum of ρ . “Average” here means averaging over states; an input state that is maximally entangled with a reference is a fairly standard proxy

$$\rho_J = \begin{pmatrix} -\epsilon_J & \theta_J = \|\cdot\| & \\ \|\cdot\| & \epsilon_J = \text{Tr}[\cdot] & \\ \theta_J & & \end{pmatrix}$$

FIG. 11. The two simple error metrics that we introduce are both derived directly from the *Jamiolkowski state*, $\rho_J(L) = (L \otimes \mathbb{1}) [|\Psi\rangle\langle\Psi|]$ of the generator [Eq. (41)]. They quantify how a generator—and the error process that it generates—would impact a computation if they were applied to part of a maximally entangled state. The Jamiolkowski probability (ϵ_J) measures the rate at which a generator transfers probability from the input state to its orthogonal complement. It is the trace of the large diagonal block shown here. The Jamiolkowski amplitude (θ_J) measures the rate at which the generator transfers amplitude from the input state to its orthogonal complement. It is the norm of either of the off-diagonal blocks shown here.

for a random input state, and there is a very close relationship between this quantity and averages over pure states of the system alone (see, e.g., Ref. [84]). The J-probability is *not* a complete description of the error. Consider, for example, the difference between (a) a dephasing process generated by pS_Z , (b) the stochastic process generated by $p/2(S_X + S_Y)$, and (c) the T_1 process generated by $p/2(S_X + S_Y + A_{X,Y})$. All three have a J-probability of p , but the actual probability of an error is input-state dependent and that dependence varies greatly over the three processes.

B. Jamiolkowski amplitude

We call the second metric the *Jamiolkowski amplitude* (or “J-amplitude” for short). It is the total amplitude created by L on the orthogonal complement to $|\Psi\rangle$ (see Fig. 11):

$$\begin{aligned} \theta_J(L) &= \|(\mathbb{1} - |\Psi\rangle\langle\Psi|) \rho_J(L) |\Psi\rangle\| \\ &= \sqrt{\langle\Psi| \rho_J(L)^2 |\Psi\rangle - \langle\Psi| \rho_J(L) |\Psi\rangle^2}. \end{aligned} \quad (44)$$

To compute the J-amplitude for elementary generators, we recall that each generator is a sum of Choi units $X_{P,Q}$ that map $\rho \rightarrow P\rho Q$. The action of a Choi unit on $|\Psi\rangle\langle\Psi|$ is simple: each Pauli maps the maximally entangled state $|\Psi\rangle$ to a distinct and orthogonal maximally entangled state. So if P and Q are both different from $\mathbb{1}$, then $P\rho Q$ is supported entirely on the orthogonal complement to $|\Psi\rangle$ and does not contribute to Eq. (44). Only Choi units where exactly one

of P or Q is $\mathbb{1}$ contribute. These terms come in pairs, as required by the Hermiticity of ρ_J , and Eq. (44) only counts the terms where $P = \mathbb{1}$ and $Q \neq \mathbb{1}$.

Unsurprisingly, $\theta_J(H_P) = 1$ for every Hamiltonian generator, H_P . Each H_P creates imaginary amplitude on a state $P|\Psi\rangle$ that is orthogonal to $|\Psi\rangle$. For every Pauli-stochastic generator, S_P , we find $\theta_J(S_P) = 0$, confirming that S_P causes only incoherent errors. The $A_{P,Q}$ generators contain [see Eq. (16)] an anticommutator term, $(i/2)\{[P, Q], \rho\}$, that creates real amplitude on the orthogonal state $(i/2)[P, Q]|\Psi\rangle$ whenever P and Q anticommute. These directly reflect the affine shift produced by the same generators (consider, as in Fig. 8, how a T_1 process shifts X eigenstates in the Z direction). So $\theta_J(A_{P,Q}) = 1$ if $\{P, Q\} = 0$, or zero otherwise. Some Pauli-correlation generators also create error amplitude. If P and Q commute, then $C_{P,Q}$ contains an anticommutator term, $-(1/2)\{[P, Q], \rho\}$, that creates real amplitude on the orthogonal state $(1/2)[P, Q]|\Psi\rangle$. So $\theta_J(C_{P,Q}) = 1$ if $[P, Q] = 0$, or zero otherwise.

Computing θ_J for a linear combination of generators is not as simple as computing ϵ_J , because amplitudes can interfere. But for generators that do not interfere—i.e., that create amplitude on mutually orthogonal states— θ_J adds in quadrature. For example, all of the Hamiltonian generators H_P induce distinct amplitudes that do not interfere, so $\theta_J(L_{\mathbb{H}}) = (\sum_P h_P^2)^{1/2} = \|\vec{h}\|$. In contrast, distinct C and A generators interfere fairly extensively. However, they all contribute exclusively *real* amplitudes, whereas Hamiltonian generators contribute exclusively imaginary amplitudes. As a result, there is no interference between (a) the net amplitude contributed by H generators and (b) the net amplitude contributed by C and A generators, and thus

$$\theta_J(L)^2 = \theta_J(L_{\mathbb{H}})^2 + \theta_J(L_C + L_A)^2. \quad (45)$$

The J-amplitude of a generator quantifies its ability to create “coherent” errors—i.e., to induce changes in an input state ρ that are orthogonal to the commutant of ρ and therefore do not change its spectrum. Unitary errors are the most obvious such errors—they *never* change the spectrum of an input state, so their impact is purely coherent. But other error generators can also produce such shifts, as seen above for the A and C generators. The resulting coherent errors behave just like those induced by unitary error processes and are captured by θ_J . As with ϵ_J , θ_J is definitely *not* a complete description of an error. For example, understanding how two coherent errors combine requires knowing their phase and direction in addition to their θ_J .

C. Discussion

We conclude this section with a brief discussion of how ϵ_J and θ_J relate to process fidelity (which can be defined

in different ways; we consider entanglement fidelity [85], diamond norm, and unitarity [86].

Fidelity and diamond norm error both compress *all* errors in an error process \mathcal{E} into a single number, but they do so in very different ways. It is more convenient to use *infidelity* ($1 - \text{fidelity}$), rather than fidelity, to quantify the size of errors. The entanglement infidelity of an error process \mathcal{E} is given by

$$\epsilon_e(\mathcal{E}) = 1 - \text{Tr}(|\Psi\rangle\langle\Psi|(\mathcal{E} \otimes \mathbb{1})[|\Psi\rangle\langle\Psi|]), \quad (46)$$

where $|\Psi\rangle$ is any maximally entangled state. So $1 - \epsilon_e$ equals the upper-left element of $\rho_J(\mathcal{E})$ when written in the basis of maximally entangled states (Fig. 11). Therefore, in the limit of small errors where $\mathcal{E} = \exp(L) \approx \mathbb{1} + L$, entanglement fidelity is determined entirely by the J-probability:

$$\epsilon_e(\mathcal{E}) = \epsilon_J + O(|L|^2). \quad (47)$$

It is often useful to expand to second order, where $\mathcal{E} = \exp(L) \approx \mathbb{1} + L + \frac{1}{2}L^2$. Doing so yields the second-order approximation

$$\begin{aligned} \epsilon_e(\mathcal{E}) &= \epsilon_J + \theta_J(L_{\mathbb{H}})^2 - \theta_J(L_C + L_A)^2 \\ &\quad - \frac{1}{2} \left(\epsilon_J^2 + \sum_P s_P^2 \right) - \sum_{P,Q} c_{P,Q}^2 + \sum_{P,Q} a_{P,Q}^2 \\ &\quad + O(|L|^3). \end{aligned} \quad (48)$$

This leading-order expansion defines the *generator infidelity* of L [36]. In the common case where coherent error rates (h_P) are much larger than stochastic error rates (s_P), so that $\epsilon_J \approx \theta_J(L_{\mathbb{H}})^2 \gg \epsilon_J^2$, it is reasonable to approximate all second-order terms *except* $\theta_J(L_{\mathbb{H}})^2$ by zero (because the $a_{P,Q}$ and $c_{P,Q}$ rates are bounded above by the s_P rates). This yields the simpler approximation

$$\epsilon_e = \epsilon_J + \theta_J^2 + O(|L_S|^2). \quad (49)$$

The diamond-norm error of a small error process is harder to approximate. Unlike fidelity, J-probability, and J-amplitude, diamond norm is defined not by an average but by a maximization over all possible input states:

$$\|\mathcal{E} - \mathbb{1}\|_{\diamond} \equiv \max_{\rho} \|(\mathcal{E} \otimes \mathbb{1} - \mathbb{1} \otimes \mathbb{1})[\rho]\|_1. \quad (50)$$

This breaks any direct connection to the Jamiolkowski state, and the resulting metric is nearly impossible to predict without numerics. The worst-case behavior of an error channel depends on its most fine-grained details (e.g., whether or not different types of error both impact the same input state). However, a useful lower bound on the diamond norm error is given by the *Jamiolkowski trace*

distance, which simply replaces the maximum over all input states with the specific case of a maximally entangled state:

$$\|\mathcal{E} - \mathbb{1}\|_{J-\text{Tr}} \equiv \|(\mathcal{E} - \mathbb{1}) \otimes \mathbb{1}[|\Psi\rangle\langle\Psi|]\|_1. \quad (51)$$

In the limit of small errors, where $\mathcal{E} \approx \mathbb{1} + L$, this is simply $\|L\|_{J-\text{Tr}} = \|\rho_J\|_1$. This expression still defies closed-form solution, but there are two interesting regimes where it is easy to approximate. First, if $\epsilon_J \gg \theta_J$, then $\|L\|_{J-\text{Tr}} \approx \epsilon_J$. Conversely, if $\theta_J \gg \epsilon_J$, then $\|L\|_{J-\text{Tr}} \approx \theta_J$. When they are of comparable magnitude, both the Jamiolkowski trace distance and the diamond norm error depend on the detailed nature of the error generator. The most notable conclusion to be drawn from this analysis is that θ_J contributes linearly to the Jamiolkowski trace distance and the diamond-norm distance, not quadratically (as it contributes to infidelity). A more detailed discussion relating the diamond norm to rates of elementary errors can be found in the supplementary information to Ref. [36].

The unitarity [86] of an error channel, u , captures the degree to which that channel preserves quantum coherence, averaged over pure states. For a purely unitary channel, $u = 1$. Using Proposition 9 in Ref. [86], which relates $u(\mathcal{E})$ to the purity of $\rho_J(\mathcal{E})$, we obtain that to leading order in L ,

$$u(e^L) = 1 - 2 \frac{d^2}{d^2 - 1} \epsilon_J + O(|L_S^2|). \quad (52)$$

We note that unitarity is entirely unaffected by coherent (Hamiltonian) errors and although A and C generators contribute at second order, their contributions are necessarily $O(|L_S^2|)$.

VIII. CONSTRUCTING REDUCED MODELS WITH ERROR GENERATORS

The preceding sections are a complete, self-contained presentation of the error generator representation. We conclude, in this section, by outlining what we see as the most exciting *application* of the error generator representation. The most obvious use of error generators is as a tool to analyze process matrices obtained from modeling, simulation, or tomography. We have used them as such, to understand estimates derived from gate set tomography [27,87] since 2017. But error generators can also be used to construct parametrized models for gate errors that are simpler, sparser, and more efficient than process matrices. We call these *reduced models*.

An N -qubit process has $4^N(4^N - 1)$ free parameters. This is an unwieldy number even for $N = 2$, and presents absurd data-storage and computation challenges for $N \gg 2$. As described above, that process can be faithfully represented by a list of the rates of elementary errors. This

representation of L is perfectly equivalent to G and has the same number of parameters.

But the error generator representation makes it easy to do something that is not possible (or at least not easy) for process matrices. We can separate the elementary generators into (1) those expected to appear and/or play a significant role in realistic noise and (2) everything else. The latter can be discarded, setting their rates to zero by fiat. The subspace of generators spanned by the remaining generators defines a *reduced model* for gate errors.

It is easy to construct reduced models using this framework. We can construct relatively generic reduced models, intended to describe any process that respects certain constraints. We can also construct specific customized models for specific quantum processors with known physics. An n -parameter reduced model for a single gate is simply a n -dimensional subspace $\mathbb{M} \subset \mathbb{L}$. The n parameters of this model are the rates (coefficients) of basis vectors (elementary generators or linear combinations of them) that span \mathbb{M} .

The easiest way to construct such a subspace is by simply making a list of elementary error generators and defining the reduced model \mathbb{M} as their span. It is also sometimes useful or necessary to include specific linear combinations of elementary error generators (e.g., $S_X + S_Y + S_Z$ for a single qubit describes depolarization). We can also construct reduced models for an entire *gate set*—a list of CPTP maps describing all the operations exposed by a processor in a common frame of reference [87]—by simply specifying an error generator in \mathbb{M} for each gate. Often, the same reduced model is used for every gate. In other cases the physics of the system suggests that different error generators should be “activated” (included in \mathbb{M}) or “frozen” (excluded from \mathbb{M}) for different gates.

A very easy way to construct reduced models is to build \mathbb{M} from entire sectors. For example, the “H+S” model,

$$\mathbb{M}_{\text{H+S}} = \mathbb{H} \oplus \mathbb{S}, \quad (53)$$

is useful for one- and two-qubit Pauli-rotation gates (\overline{G} is a Pauli rotation if $\overline{G}[\rho] = e^{-i\theta P} \rho e^{i\theta P}$ for some Pauli P). It can model all unitary errors (including over- or under-rotations as well as “tilt” errors that change the rotation axis of the gate) and the most common stochastic errors including depolarization and dephasing in the eigenbasis of the gate (as is produced, e.g., by fluctuating over- or under-rotation). For a single qubit, this model has $2 \times$ fewer parameters than a full CPTP map; for two qubits, it is $8 \times$ more efficient.

For processors with $N > 1$ qubits, generator space can be partitioned further. This fine-grained partition becomes increasingly useful as N grows. We partition each sector ($\mathbb{H}, \mathbb{S}, \mathbb{C}, \mathbb{A}$) by the *weight* and *support* of its elementary generators [see Fig. 2(c)]. These are defined as follows:

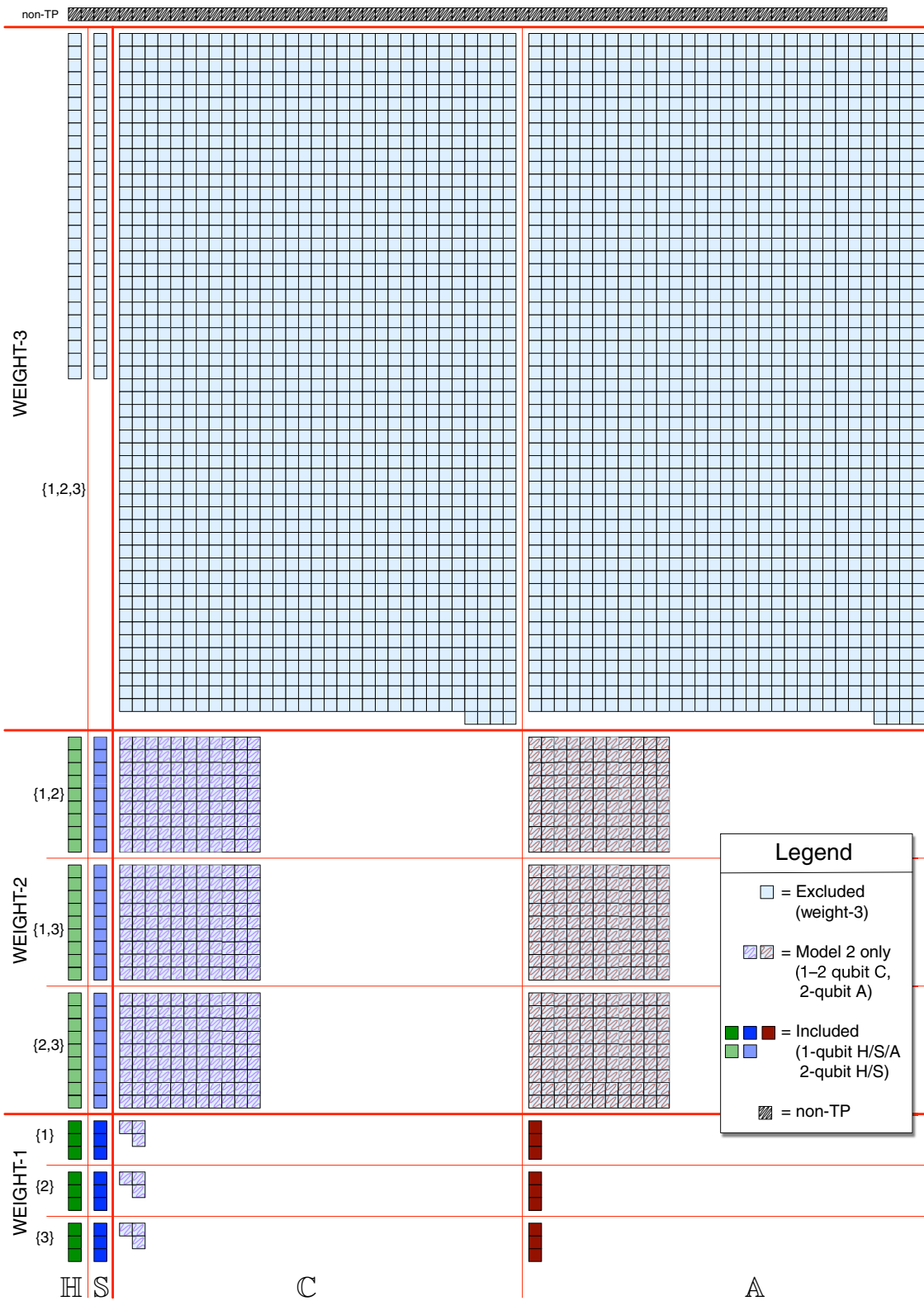


FIG. 12. For a generic three-qubit error process, this figure illustrates the relative sizes of the \mathbb{H} , \mathbb{S} , \mathbb{C} , and \mathbb{A} sectors and subsectors of its error generator space. Each small box represents one of the 4096 elements in a 64×64 process matrix: 64 are constrained by trace preservation, leaving 4032 free parameters. More than 83% of these ($27 + 27 + 1647 + 1647 = 3348$) are weight-3. They are excluded from both the “weight ≤ 2 ” and “ $\mathbb{H}2+\mathbb{S}2+\mathbb{A}1$ ” models described in the text. Another 15% ($297+297+9=594$) are \mathbb{C} and weight-2 \mathbb{A} -type generators. These are excluded from “ $\mathbb{H}2+\mathbb{S}2+\mathbb{A}1$.” The remaining 81 generators in the “ $\mathbb{H}2+\mathbb{S}2+\mathbb{A}1$ ” model constitute just 2% of the full generator space, but they represent most phenomena appearing in physical models of error.

- (1) The *support* of Pauli operator P is the set of qubits on which it acts nontrivially.
- (2) The support of a generator H_P or S_P is the support of P .
- (3) The support of a generator $C_{P,Q}$ or $A_{P,Q}$ is the union of the supports of P and Q .
- (4) The *weight* of a generator is the number of qubits in its support.

Each elementary generator can be unambiguously labeled by its support (and thus its weight). We can then partition each sector into N distinct subsectors of fixed weight $w = 1 \dots N$. We refer to these subsectors as \mathbb{H}_w , \mathbb{S}_w , \mathbb{C}_w , and \mathbb{A}_w , respectively. If desired, we can partition each of those subsectors into $\binom{N}{w}$ subsectors of fixed support \mathbb{Q} .

This fine-grained partition of generator space provides a great deal of flexibility to construct models that (1) respect either general locality principles or specific physical modeling assumptions and (2) have relatively few parameters. These models form a lattice, bookended by the “full CPTP model” \mathbb{L} and the “target model” \emptyset . Exploring this lattice in detail is beyond the scope of this paper, but here (and illustrated in Fig. 12) are a few examples that suggest the framework’s potential:

- (1) *The two-qubit “H+S+A1” model.* This is a reduced model for two-qubit subsystems that incorporates all the errors (including crosstalk and T_1 decay) predicted by most theory models. It includes the entire \mathbb{H} and \mathbb{S} sectors on both qubits (15 parameters each) and the weight-1 \mathbb{A}_1 subsector required to model local amplitude-damping errors on both qubits ($3 + 3 = 6$ parameters). This model has 36 parameters, compared to the 240 required for a process matrix.
- (2) *All weight ≤ 2 errors on N qubits.* A reasonable ansatz for a single circuit layer of nonentangling gates on an N -qubit processor is that no three-body couplings exist and therefore that the dynamics can be well approximated by local (weight-1) and two-qubit (weight-2) errors. This suggests a reduced model $\mathbb{M} = \mathbb{H}_1 \oplus \mathbb{H}_2 \oplus \mathbb{S}_1 \oplus \mathbb{S}_2 \oplus \mathbb{C}_1 \oplus \mathbb{C}_2 \oplus \mathbb{A}_1 \oplus \mathbb{A}_2$. It contains 12 weight-1 error generators on each qubit and 216 weight-2 error generators on each pair, for a total of $108N^2 - 96N$ parameters. This is a nontrivial number but for $N = 10$ qubits, $\dim(\mathbb{M})$ is only 9840, which is tractable on modern computers. A ten-qubit CPTP map has just over 10^{12} parameters, which is not tractable.
- (3) *The N -qubit “H2+S2+A1” model.* We can combine the virtues of the previous two models to get a more efficient N -qubit model that excludes Pauli-correlation and weight-2 active error generators. This model is formally given by $\mathbb{M} = \mathbb{H}_1 \oplus \mathbb{H}_2 \oplus \mathbb{S}_1 \oplus \mathbb{S}_2 \oplus \mathbb{A}_1$. It contains nine weight-1 error

generators on each qubit and 18 weight-2 error generators on each pair, for a total of $9N^2$ parameters. For $N = 20$ qubits, it has 3249 parameters.

These models are examples but, more importantly, they are starting points. Given any specific architecture, it is easy to point out specific errors that are likely to occur in that system but not included in the models above. But it is even easier to choose and add $O(1)$ elementary error generators to the model, enabling it to model that effect without increasing its complexity very much.

IX. CONCLUSIONS

In this paper, we combine some previously known ideas—e.g., small-error processes [42] and generators of dynamical maps [45,88–91]—with a new classification into four physically distinct sectors, to produce the first comprehensive classification of Markovian errors. This taxonomy applies equally well to single-qubit gates and to circuit layers on five, 53, or 1000 qubits. It classifies *all* Markovian errors. Our analysis makes it possible to (1) analyze experimentally reconstructed logic gates and dissect their errors into distinct components with simple physical interpretations and (2) construct simple polynomially-sized parametrized error models for N qubits by combining tailored subsets of those components. This framework is inspired in large part by the demands of experimental tomography (see, e.g., Refs. [27,36,92–96]), but also by the investigation of single qubit processes in Ref. [66].

These practical applications of error generator analysis have been demonstrated in experiments [36]. Physically motivated reduced models constructed using error generators may—finally—make it not just possible but *easy* to comprehensively describe, measure, and reconstruct the real-world dynamics of N -qubit systems for $N \gg 1$. As the size and fidelity of quantum processors grows and fault-tolerant quantum error correction becomes feasible, the need for detailed characterization and measurement of error budgets grows too. The techniques presented here provide a foundation for building the characterization protocols and detailed error metrics required to enable and validate qubit hardware for fault-tolerant quantum computing.

ACKNOWLEDGMENTS

This work was supported by the U.S. Department of Energy, Office of Science, Office of Advanced Scientific Computing Research Quantum Testbed Program and by the Office of the Director of National Intelligence (ODNI), Intelligence Advanced Research Projects Activity (IARPA). M.P.S. was partially funded by LPS/ARO Grant No. W911NF-14-C-0048 (while employed at Raytheon BBN Technologies). R.B.-K. thanks Ivan Deutsch for

pointing out Ref. [42]. Sandia National Laboratories is a multimission laboratory managed and operated by National Technology and Engineering Solutions of Sandia, LLC., a wholly owned subsidiary of Honeywell International, Inc., for the U.S. Department of Energy's National Nuclear Security Administration under Contract No. DE-NA-0003525. All statements of fact, opinion, or conclusions contained herein are those of the authors and should not be construed as representing the official views or policies of IARPA, the ODNI, the U.S. Department of Energy, or the U.S. Government.

-
- [1] J.-M. Reiner, S. Zanker, I. Schwenk, J. Leppäkangas, F. Wilhelm-Mauch, G. Schön, and M. Marthaler, Effects of gate errors in digital quantum simulations of fermionic systems, *Quantum Sci. Technol.* **3**, 045008 (2018).
- [2] D. Willsch, M. Nocon, F. Jin, H. De Raedt, and K. Michielsen, Gate-error analysis in simulations of quantum computers with transmon qubits, *Phys. Rev. A* **96**, 062302 (2017).
- [3] T. Proctor, K. Rudinger, K. Young, E. Nielsen, and R. Blume-Kohout, Measuring the capabilities of quantum computers, *Nat. Phys.* **18**, 75 (2021).
- [4] K. Georgopoulos, C. Emary, and P. Zuliani, arXiv (2021), [ArXiv:2101.02109](https://arxiv.org/abs/2101.02109).
- [5] R. Rines, K. Obenland, and I. Chuang, arXiv (2019), [ArXiv:1905.10724](https://arxiv.org/abs/1905.10724).
- [6] S. S. Elder, C. S. Wang, P. Reinhold, C. T. Hann, K. S. Chou, B. J. Lester, S. Rosenblum, L. Frunzio, L. Jiang, and R. J. Schoelkopf, High-Fidelity Measurement of Qubits Encoded in Multilevel Superconducting Circuits, *Phys. Rev. X* **10**, 011001 (2020).
- [7] C. K. Andersen, A. Remm, S. Lazar, S. Krinner, N. Lacroix, G. J. Norris, M. Gabureac, C. Eichler, and A. Wallraff, arXiv (2019), [ArXiv:1912.09410](https://arxiv.org/abs/1912.09410).
- [8] A. Bermudez, X. Xu, M. Gutiérrez, S. C. Benjamin, and M. Müller, Fault-tolerant protection of near-term trapped-ion topological qubits under realistic noise sources, *Phys. Rev. A* **100**, 062307 (2019).
- [9] M. Gong, *et al.*, arXiv (2019), [ArXiv:1907.04507](https://arxiv.org/abs/1907.04507).
- [10] C. C. Bultink, T. E. O'Brien, R. Vollmer, N. Muthusubramanian, M. W. Beekman, M. A. Rol, X. Fu, B. Tarasinski, V. Ostroukh, B. Varbanov, A. Bruno, and L. DiCarlo, arXiv (2019), [ArXiv:1905.12731](https://arxiv.org/abs/1905.12731).
- [11] V. Negnevitsky, M. Marinelli, K. K. Mehta, H.-Y. Lo, C. Flühmann, and J. P. Home, Repeated multi-qubit readout and feedback with a mixed-species trapped-ion register, *Nature* **563**, 527 (2018).
- [12] C. J. Trout, M. Li, M. Gutiérrez, Y. Wu, S.-T. Wang, L. Duan, and K. R. Brown, Simulating the performance of a distance-3 surface code in a linear ion trap, *New J. Phys.* **20**, 043038 (2018).
- [13] M. Takita, A. W. Cross, A. D. Córcoles, J. M. Chow, and J. M. Gambetta, Experimental Demonstration of Fault-Tolerant State Preparation with Superconducting Qubits, *Phys. Rev. Lett.* **119**, 180501 (2017).
- [14] M. Takita, A. D. Córcoles, E. Magesan, B. Abdo, M. Brink, A. Cross, J. M. Chow, and J. M. Gambetta, Demonstration of Weight-Four Parity Measurements in the Surface Code Architecture, *Phys. Rev. Lett.* **117**, 210505 (2016).
- [15] A. D. Córcoles, E. Magesan, S. J. Srinivasan, A. W. Cross, M. Steffen, J. M. Gambetta, and J. M. Chow, Demonstration of a quantum error detection code using a square lattice of four superconducting qubits, *Nat. Commun.* **6**, 6979 (2015).
- [16] J. M. Chow, J. M. Gambetta, E. Magesan, D. W. Abraham, A. W. Cross, B. R. Johnson, N. A. Masluk, C. A. Ryan, J. A. Smolin, S. J. Srinivasan, and M. Steffen, Implementing a strand of a scalable fault-tolerant quantum computing fabric, *Nat. Commun.* **5**, 4015 (2014).
- [17] R. Barends, *et al.*, Superconducting quantum circuits at the surface code threshold for fault tolerance, *Nature* **508**, 500 (2014).
- [18] D. G. Cory, M. D. Price, W. Maas, E. Knill, R. Laflamme, W. H. Zurek, T. F. Havel, and S. S. Somaroo, Experimental Quantum Error Correction, *Phys. Rev. Lett.* **81**, 2152 (1998).
- [19] K. Wright, *et al.*, Benchmarking an 11-qubit quantum computer, *Nat. Commun.* **10**, 5464 (2019).
- [20] A. Bermudez, X. Xu, R. Nigmatullin, J. O'Gorman, V. Negnevitsky, P. Schindler, T. Monz, U. G. Poschinger, C. Hempel, J. Home, F. Schmidt-Kaler, M. Biercuk, R. Blatt, S. Benjamin, and M. Müller, Assessing the Progress of Trapped-Ion Processors Towards Fault-Tolerant Quantum Computation, *Phys. Rev. X* **7**, 041061 (2017).
- [21] L. Egan, D. M. Debroy, C. Noel, A. Risinger, D. Zhu, D. Biswas, M. Newman, M. Li, K. R. Brown, M. Cetina, and C. Monroe, Fault-tolerant control of an error-corrected qubit, *Nature* **598**, 281 (2021).
- [22] E. Magesan, D. Puzzioli, C. E. Granade, and D. G. Cory, Modeling quantum noise for efficient testing of fault-tolerant circuits, *Phys. Rev. A* **87**, 012324 (2013).
- [23] Y. Tomita and K. M. Svore, Low-distance surface codes under realistic quantum noise, *Phys. Rev. A* **90**, 062320 (2014).
- [24] M. Gutiérrez, L. Svec, A. Vargo, and K. R. Brown, Approximation of realistic errors by Clifford channels and Pauli measurements, *Phys. Rev. A* **87**, 030302(R) (2013).
- [25] A. K. Pal, P. Schindler, A. Erhard, Á. Rivas, M.-A. Martin-Delgado, R. Blatt, T. Monz, and M. Müller, arXiv (2020), [ArXiv:2012.07911](https://arxiv.org/abs/2012.07911).
- [26] Google Quantum AI, *Nature* **595**, 383 (2021).
- [27] R. Blume-Kohout, J. K. Gamble, E. Nielsen, K. Rudinger, J. Mizrahi, K. Fortier, and P. Maunz, Demonstration of qubit operations below a rigorous fault tolerance threshold with gate set tomography, *Nat. Commun.* **8**, 14485 (2017).
- [28] P. Murali, J. M. Baker, A. J. Abhari, F. T. Chong, and M. Martonosi, arXiv (2019), [ArXiv:1901.11054](https://arxiv.org/abs/1901.11054).
- [29] D. Bultrini, M. H. Gordon, E. López, and G. Sierra, arXiv (2020), [ArXiv:2012.00831](https://arxiv.org/abs/2012.00831).
- [30] J. Hu, Q. Liang, N. Rengaswamy, and R. Calderbank, arXiv (2020), [ArXiv:2011.00197](https://arxiv.org/abs/2011.00197).
- [31] S. Endo, S. C. Benjamin, and Y. Li, Practical Quantum Error Mitigation for Near-Future Applications, *Phys. Rev. X* **8**, 031027 (2018).
- [32] C. Song, J. Cui, H. Wang, J. Hao, H. Feng, and Y. Li, Quantum computation with universal error mitigation on a

- superconducting quantum processor, *Sci. Adv.* **5**, eaaw5686 (2019).
- [33] S. S. Tannu and M. K. Qureshi, arXiv (2018), [ArXiv:1805.10224](#).
- [34] D. C. Murphy and K. R. Brown, Controlling error orientation to improve quantum algorithm success rates, *Phys. Rev. A* **99**, 032318 (2019). [ArXiv:1810.07813](#)
- [35] I. L. Chuang and M. A. Nielsen, Prescription for experimental determination of the dynamics of a quantum black box, *J. Mod. Opt.* **44**, 2455 (1997).
- [36] M. T. Madzik, S. Asaad, A. Youssry, B. Joecker, K. M. Rudinger, E. Nielsen, K. C. Young, T. J. Proctor, A. D. Baczewski, A. Laucht, V. Schmitt, F. E. Hudson, K. M. Itoh, A. M. Jakob, B. C. Johnson, D. N. Jamieson, A. S. Dzurak, C. Ferrie, R. Blume-Kohout, and A. Morello, Precision tomography of a three-qubit donor quantum processor in silicon, *Nature* **601**, 348 (2022).
- [37] H.-P. Breuer, E.-M. Laine, J. Piilo, and B. Vacchini, Colloquium: Non-Markovian dynamics in open quantum systems, *Rev. Mod. Phys.* **88**, 021002 (2016).
- [38] D. Aharonov, A. Kitaev, and N. Nisan, in *Proceedings of the Thirtieth Annual ACM Symposium on Theory of Computing*, STOC '98 (Association for Computing Machinery, New York, NY, USA, 1998), p. 20.
- [39] We see no obstacle to constructing a version of our framework for systems of Hilbert-space dimension $d \neq 2^N$ but many of the details would need to be done in different ways because we make heavy use of (1) the Pauli basis and (2) underlying locality assumptions intrinsic to N qubits.
- [40] An N -qubit density matrix ρ written in the Pauli basis is a column vector $|\rho\rangle\rangle$ with elements $\langle\langle P|\rho\rangle\rangle = \text{Tr}(P\rho)$.
- [41] A cone is a subset of a vector space that is closed under positive linear combinations.
- [42] A. N. Korotkov, arXiv (2013), [ArXiv:1309.6405](#).
- [43] A. V. Rodionov, A. Veitia, R. Barends, J. Kelly, D. Sank, J. Wenner, J. M. Martinis, R. L. Kosut, and A. N. Korotkov, Compressed sensing quantum process tomography for superconducting quantum gates, *Phys. Rev. B Condens. Matter* **90**, 144504 (2014).
- [44] *Proof*: Because $\mathcal{E} \approx \mathbb{1}$, all eigenvalues of \mathcal{E} are close to 1, and thus nonzero and non-negative. Thus \mathcal{E} is invertible and has no negative eigenvalues. So by Theorem 3.4 in [97] (see also Ref. [98]), \mathcal{E} has a real logarithm, which is necessarily the principal branch of $\log \mathcal{E}$.
- [45] G. Lindblad, On the generators of quantum dynamical semigroups, *Commun. Math. Phys.* **48**, 119 (1976).
- [46] J. J. Wallman, Randomized benchmarking with gate-dependent noise, *Quantum* **2**, 47 (2018).
- [47] There is physics behind this math too. Any stochastic X or Y error generated continuously during this π gate gets “twirled” into a perfectly equal mixture of X and Y errors. So there really is no during-gate generator that can produce a biased mixture of X and Y errors afterward.
- [48] A semialgebra is like an algebra but restricted to a cone.
- [49] The solid tangent cone to a convex set X , at a point x on its boundary, is the closure of the cone formed by all rays from x through a distinct point in X .
- [50] We denote the set of *distinct* pairs of distinct Pauli operators as $\{(P, Q > P)\}$, to indicate that only one of (P, Q) or (Q, P) is included.
- [51] N. Johnston and D. W. Kribs, Quantum gate fidelity in terms of Choi matrices, *J. Phys. A: Math. Theor.* **44**, 495303 (2011).
- [52] M.-D. Choi, Completely positive linear maps on complex matrices, *Linear Algebra Appl.* **10**, 285 (1975).
- [53] This does not imply that whenever \mathcal{E} is a mixture of unitaries, $\log \mathcal{E}$ is strictly a linear combination of H , S , and C generators. Rather, if $|J_k| = O(\epsilon)$ for each J_k in Eq. (11), then expansion of $\log \mathcal{E}$ or $\mathcal{E} - \mathbb{1}$ to $O(\epsilon^2)$ can be written entirely in terms of H , S , and C generators. Other terms (the A -type generators discussed below) can and do appear at order ϵ^3 .
- [54] M. B. Ruskai, S. Szarek, and E. Werner, An analysis of completely-positive trace-preserving maps on M_2 , *Linear Algebra Appl.* **347**, 159 (2002).
- [55] Technically, \vec{h} is a *pseudovector*, since it defines a rotation. The affine rates, discussed a bit lower down, form a true vector. This distinction is irrelevant as long as everyone involved has the courtesy and common sense to avoid performing antiunitary coordinate changes.
- [56] B. Eastin, Ph.D. thesis, University of New Mexico (2007).
- [57] S. T. Flammia and Y.-K. Liu, Direct Fidelity Estimation from Few Pauli Measurements, *Phys. Rev. Lett.* **106**, 230501 (2011).
- [58] A. Chiuri, V. Rosati, G. Vallone, S. Pádua, H. Imai, S. Giacomini, C. Macchiavello, and P. Mataloni, Experimental Realization of Optimal Noise Estimation for a General Pauli Channel, *Phys. Rev. Lett.* **107**, 253602 (2011).
- [59] M. Gutiérrez and K. R. Brown, Comparison of a quantum error-correction threshold for exact and approximate errors, *Phys. Rev. A* **91**, 022335 (2015).
- [60] D. K. Tuckett, S. D. Bartlett, and S. T. Flammia, Ultra-high Error Threshold for Surface Codes with Biased Noise, *Phys. Rev. Lett.* **120**, 050505 (2018).
- [61] S. J. Beale, J. J. Wallman, M. Gutiérrez, K. R. Brown, and R. Laflamme, Quantum Error Correction Decoheres Noise, *Phys. Rev. Lett.* **121**, 190501 (2018).
- [62] E. Huang, A. C. Doherty, and S. Flammia, Performance of quantum error correction with coherent errors, *Phys. Rev. A* **99**, 022313 (2019).
- [63] S. T. Flammia and J. J. Wallman, arXiv (2019), [ArXiv:1907.12976](#).
- [64] R. Harper, W. Yu, and S. T. Flammia, arXiv (2020), [ArXiv:2007.07901](#).
- [65] It can be constructed as $\mathcal{U}\Gamma_{1 \rightarrow 0}\mathcal{U}^\dagger$, where $\mathcal{U}[\cdot] = U \cdot U^\dagger$ for a suitable unitary U .
- [66] R. Kueng, D. M. Long, A. C. Doherty, and S. T. Flammia, Comparing Experiments to the Fault-Tolerance Threshold, *Phys. Rev. Lett.* **117**, 170502 (2016).
- [67] K. M. Audenaert and S. Scheel, On random unitary channels, *New J. Phys.* **10**, 023011 (2008).
- [68] So inferring the precise cause of a given error generator is generally not justified.
- [69] P. Busch and P. Lahti, in *Compendium of Quantum Physics* (Springer, 2009), p. 356.
- [70] S. Aaronson and D. Gottesman, Improved simulation of stabilizer circuits, *Phys. Rev. A* **70**, 052328 (2004).
- [71] H. Zhu, R. Kueng, M. Grassl, and D. Gross, arXiv (2016), [ArXiv:1609.08172](#).

- [72] E. Magesan, J. M. Gambetta, and J. Emerson, Scalable and Robust Randomized Benchmarking of Quantum Processes, *Phys. Rev. Lett.* **106**, 180504 (2011).
- [73] C. Dankert, R. Cleve, J. Emerson, and E. Livine, Exact and approximate unitary 2-designs and their application to fidelity estimation, *Phys. Rev. A* **80**, 012304 (2009).
- [74] For a more careful and context-aware discussion of this constraint, see Sec. VI.
- [75] Setting aside the purely unitary errors, which are capably described by H generators.
- [76] This (finally) is the motivation for the “active” moniker.
- [77] D. W. Leung, Choi’s proof as a recipe for quantum process tomography, *J. Math. Phys.* **44**, 528 (2003).
- [78] This is just one stage in a beautiful hierarchy of divisibility conditions outlined in Ref. [81]. There are also *indivisible* processes, which cannot be nontrivially decomposed at all into $\mathcal{E} = \mathcal{E}_1 \circ \mathcal{E}_2$.
- [79] M. M. Wolf, J. Eisert, T. S. Cubitt, and J. I. Cirac, Assessing Non-Markovian Quantum Dynamics, *Phys. Rev. Lett.* **101**, 150402 (2008).
- [80] *Proof*: If $t > 1$ then $e^{tL} = \mathcal{E}^{\lfloor t \rfloor} e^{(t \bmod 1)L}$. Since any channel \mathcal{E} is contractive, the amount by which e^{tL} violates CP cannot exceed that of $e^{(t \bmod 1)L}$.
- [81] M. M. Wolf and J. I. Cirac, Dividing quantum channels, *Commun. Math. Phys.* **279**, 147 (2008).
- [82] A. Gilchrist, N. K. Langford, and M. A. Nielsen, Distance measures to compare real and ideal quantum processes, *Phys. Rev. A* **71**, 062310 (2005).
- [83] A. Jamiolkowski, Linear transformations which preserve trace and positive semidefiniteness of operators, *Rep. Math. Phys.* **3**, 275 (1972).
- [84] M. A. Nielsen, A simple formula for the average gate fidelity of a quantum dynamical operation, *Phys. Lett. A* **303**, 249 (2002).
- [85] H. Barnum, M. A. Nielsen, and B. Schumacher, Information transmission through a noisy quantum channel, *Phys. Rev. A* **57**, 4153 (1998).
- [86] J. Wallman, C. Granade, R. Harper, and S. T. Flammia, Estimating the coherence of noise, *New J. Phys.* **17**, 113020 (2015).
- [87] E. Nielsen, J. K. Gamble, K. Rudinger, T. Scholten, K. Young, and R. Blume-Kohout, Gate set tomography, *Quantum* **5**, 557 (2021).
- [88] B. Bellomo, A. De Pasquale, G. Gualdi, and U. Marzolino, Reconstruction of Markovian master equation parameters through symplectic tomography, *Phys. Rev. A* **80**, 052108 (2009).
- [89] S. G. Schirmer and D. K. L. Oi, Quantum system identification by Bayesian analysis of noisy data: Beyond Hamiltonian tomography, *Laser Phys.* **20**, 1203 (2010).
- [90] F. A. Pollock and K. Modi, Tomographically reconstructed master equations for any open quantum dynamics, *Quantum* **2**, 76 (2018).
- [91] A. A. Gentile, B. Flynn, S. Knauer, N. Wiebe, S. Paesani, C. E. Granade, J. G. Rarity, R. Santagati, and A. Laing, arXiv (2020), [ArXiv:2002.06169](https://arxiv.org/abs/2002.06169).
- [92] D. Kim, D. R. Ward, C. B. Simmons, J. K. Gamble, R. Blume-Kohout, E. Nielsen, D. E. Savage, M. G. Lagally, M. Friesen, S. N. Coppersmith, and M. A. Eriksson, Microwave-driven coherent operation of a semiconductor quantum dot charge qubit, *Nat. Nanotechnol.* **10**, 243 (2015).
- [93] J. P. Dehollain, J. T. Muhonen, R. Blume-Kohout, K. M. Rudinger, J. K. Gamble, E. Nielsen, A. Laucht, S. Simmons, R. Kalra, A. S. Dzurak, and A. Morello, Optimization of a solid-state electron spin qubit using gate set tomography, *New J. Phys.* **18**, 103018 (2016).
- [94] S. Mavadia, C. L. Edmunds, C. Hempel, H. Ball, F. Roy, T. M. Stace, and M. J. Biercuk, Experimental quantum verification in the presence of temporally correlated noise, *npj Quantum Inf.* **4**, 7 (2018).
- [95] M. Ware, G. Ribeill, D. Ristè, C. A. Ryan, B. Johnson, and M. P. da Silva, arXiv (2018), [ArXiv:1803.01818](https://arxiv.org/abs/1803.01818).
- [96] A. C. Hughes, V. M. Schäfer, K. Thirumalai, D. P. Nadlinger, S. R. Woodrow, D. M. Lucas, and C. J. Ballance, arXiv (2020), [ArXiv:2004.08162](https://arxiv.org/abs/2004.08162).
- [97] J. Gallier, arXiv preprint [arXiv:0805.02452008](https://arxiv.org/abs/0805.02452008).
- [98] N. J. Higham, *Functions of Matrices: Theory and Computation* (SIAM, Philadelphia, PA, 2008).